SUSTAINABLE INCORPORATION OF WASTE GRANITE DUST AS PARTIAL REPLACEMENT OF SAND IN AUTOCLAVE AERATED CONCRETE

By

Muhammad Saeed Zafar

(00000171360)

A thesis submitted in partial fulfillment of the requirements for the degree of **Master of Science in Structural Engineering**

NUST Institute of Civil Engineering (NICE)

National University of Sciences and Technology

Islamabad, Pakistan

(2019)

This is to certify

that Thesis titled

SUSTAINABLE INCORPORATION OF WASTE GRANITE DUST AS PARTIAL REPLACEMENT OF SAND IN AUTOCLAVE AERATED CONCRETE

Submitted by

Muhammad Saeed Zafar

Has been accepted towards the partial fulfillment

of

the requirements

for award of degree of

Master of Science in Structural Engineering

Thesis Supervisor

_____

Dr. Rao Arsalan Khushnood, PhD
Assistant Professor
Department of Structural Engineering
NUST Institute of Civil Engineering (NICE)

School of Civil and Environmental Engineering (SCEE)
National University of Sciences and Technology (NUST)

May 2019, Islamabad Pakistan

THESIS ACCEPTANCE CERTIFICATE

Certified that final copy of MS/MPhill thesis written by Mr Mmuhammad Saeed Zafar, Registration No. 00000171360, of MS Structural Engineering 2016 Batch (NICE) has been vetted by undersigned, found completed in all respects as per NUST Statutes/Regulations, is free of plagiarism, errors, and mistakes and is accepted as partial fulfilment for award of MS/MPhil degree. It is further certified that necessary amendments as pointed out by GEC members of the scholar have been incorporated in the said thesis.

Signature_____

Name of Supervisor: Dr. Rao Arsalan Khushnood

Date: _____

Signature (HoD)_____

Date: _____

Signature Dean/Principal)_____

Date:_____

DEDICATED

TO

HOLY PROPHET (P.B.U.H)

AND

MY LOVING PARENTS &TEACHERS

WHO GAVE ME A LOT OF INSPIRATION

&

COURAGE

ACKNOWLEDGEMENTS

All praise to Almighty Allah who gave the courage and power to the author for completing this research work.

I am thankful to my supervisor Dr. Rao Arsalan Khushnood, HoD Structural engineering department, NUST Institute of Civil Engineering (NICE) for giving me time and support from initial to final level, made it possible for me to complete this work. His able guidance and encouragement steered me to think beyond visible facts to bring more useful and applicable conclusions from the work in hand. His pleasant and friendly conduct facilitated me to discuss my view point on the subject in detail and addressed my queries to my entire satisfaction.

I must not forget the supporting role of my friends and especially Engr Waqas Siddique, Engr. Usman Javed, Engr. Tayyab Zafar, Engr. Haseeb Taj, Engr. Asif Ali and laboratory staff at NICE, for providing the technical assistance and cooperation during the reported research work.

Lastly, I want to thanks my parents and family members for supporting me in all phases of life.

ABSTRACT

Solid waste management is major environmental challenge over the globe. The foremost source of total solid waste production is the waste generated from the granite processing industries due to its abundance. This waste could be valuable if properly used as partial replacement of sand in concrete which will minimize the environmental risks. Moreover this could meet the increasing demand of sand in construction industry which is leading to the depletion of natural sand resources. This research studied the properties of autoclave aerated concrete (AAC) containing waste granite dust from granite industrial waste. Waste granite dust was incorporated as sand replacement (0%, 5%, 10%, 15% & 20%). The microscopic characteristics of waste granite powder were evaluated by Scanning Electron Microscopy (SEM), X-ray Diffraction (XRD) and Thermo-gravimetric analysis (TGA) and particle size analysis. The mechanical properties of AAC containing waste granite dust were examined by conducting water absorption, unit weight, compressive strength and flexure strength. For microstructure of AAC containing granite waste powder, SEM, XRD and TGA were performed. Thermal properties and durability of AAC was examined by thermal conductivity and acid attack test. The test results showed that the addition of waste granite dust improved the mechanical, microstructural and thermal properties of AAC. The optimum replacement was observed as 20%. Test results showed that water absorption decreased while density and thermal conductivity increased with increase in waste granite powder percentage up to 20%. Compressive strength was 9.696 MPa at 20% replacement which is very close to the strength of first class brick. Weight loss and Strength loss against sulfuric acid attack is observed more as compared to hydrochloric acid attack which is due to the more destructive nature of sulfuric acid. The scanning electron microscopy and thermogravimetric analysis endorsed the occurrence of pozzolanic activity due to addition of waste granite powder which significantly improved the microstructure by pore filling and tobermorite formation. Conclusively, the use of waste granite dust as partial replacement of sand in autoclave aerated concrete is justified.

TABLE OF CONTENTS

LIST OF TABLES

LIST OF FIGURES

CHAPTER 1: INTRODUCTION

1.1. General

Planet earth is facing serious depletion of resources due to increased demand of available natural resources. Natural sand resources are depleting due to enhanced demand of concrete. Wiedmann et al. (2015) stated that around 70 billion tonnes global materials extraction occurred in year 2008, whereas construction materials contributed 29.58 billion tonnes/year. River sand consumption can be reduced by replacing some proportion of sand with industrial waste granite dust. Autoclave aerated concrete may be an option to reduce the consumption of sand by introducing pores and partially replacing sand with waste granite dust. The waste granite dust otherwise generate atmosphere cloudy, smoggy and leads to serious cardio-respiratory diseases. Also the disposal of granite waste has become an uneconomical due to unavailability of dumping sites especially in urban areas. The large amount of dusty, solid and sludge waste is generated as by product of stone industry. Granite waste dust is one of the waste of stone industry, which is obtained after cutting, grinding and polishing of raw granite for commercial production of granite products. However, the powdered waste dust and sludge(dried form) may transform into suspended particulate matter (particle size less than 363 micron can easily get air borne) (Lakhani et al., 2014) causing serious air pollution and poses several environmental hazards (Rego et al., 2001). These suspended dust particles may cause several skin, ocular and respiratory diseases (Pareek, 2007; Rego et al., 2001; Saboya Jr et al., 2007) and decrease average human life expectancy residing within vicinity. Furthermore, if the granite sludge produced during the processing of stone is deposited for long period in dumping areas, chances of vegetation reduce in that specific area and degradation of soil will occur. Moreover, the granite dust also contain very fine particles which may significantly disturb the availability of underground water and ultimately affect the flow regime of aquifers (Lakhani et al., 2014).

Autoclave aerated concrete is a type of lightweight concrete containing air voids being generated by the reaction of added aluminum with quick lime and water during cement slurry mixing. It has lower hardened density, shrinkage, comparatively higher thermal resistivity and heat resistance than normal concrete (Dey et al., 2014) (Aroni, 1990) . AAC is eco-friendly building material due to low energy and material consumption during its manufacturing and production phases respectively (Mostafa, 2005). After

unmolding the hardened AAC, it is used to be steam cured at elevated temperature between 180 and 200ºC (HFW., 1997.) and pressure of 4-16 MPa for 8-16 hours (Hamad, 2014) to achieve its 28 days strength within first few hours. Generally, AAC is produced from cement, sand, lime as major constituents and aluminum powder as pore forming agent (Kurama et al., 2009). Therefore, aluminum powder reacts with lime and water releasing hydrogen gas bubbles in cement slurry to form aerated concrete (Short A, 1963). A. M. Neville and J. J. Brooks (2010) reported the chemical reaction occurs between the aluminum powder and lime in presence of water, bubbling off the hydrogen gas in fresh concrete state.

$$2Al + 3Ca(OH)2 + 6H2O \rightarrow 3CaOAl2O3.6H2O + 3H2 \uparrow$$

During autoclaving process, high temperature and pressure alters the chemistry of hydration such as calcium silicate hydrate transforms to crystalline calcium silicate hydrate, therefore, amorphous silica may generate tobermorite crystals on heating, thus to enhance the mechanical properties (H, 2007). Whereas, granite chemically rich in amorphous silica (Asadi Shamsabadi et al., 2018) may increase the concentration of tobermorite crystals due to induced pozzolanic activity of incorporated granite powder in AAC. Ramos et al. (2013) reported that the chemical composition of waste granite powder meets the requirements [(Silica + Alumina + Iron oxide) > 70%] of (ASTM-C618) to be considered as a pozzolanic material.

Several researchers investigated the mechanical, thermal and durability properties of AAC incorporating agro-industrial wastes as replacement of river sand, such as perlite (Różycka, 2016), coal bottom ash (Wongkeo and Chaipanich, 2010), fly ash (Narayanan, 2000), slag (Mostafa, 2005) and zeolite (Albayrak et al., 2007) as high quartz sand replacement in AAC. Moreover, various researchers such as Felixkala (2010), Hamza (2011), A. Arivumangai1 (2014), Gupta and Vyas (2018), Sadek (2016), Singh (2016) and Ghannam et al. (2016) have incorporated granite waste as fine aggregate replacement in cement concrete.

Conclusively, this study is pioneer effort of sustainable incorporation of waste granite dust as river sand replacement in autoclave aerated concrete. In this research, granite waste dust has been characterized as macro and micro level to assess its suitability as fine aggregates in AAC. Waste granite dust incorporated concrete was tested for shrinkage response and air content in fresh state. In hardened state, it was evaluated for compressive

strength, flexure strength, hardened density, porosity and water absorption. For durability properties,WGD incorporated AAC was tested for weight loss using 5% hydrochloric acid and sulfuric acid solution respectively. Microstructural and supplementary analysis was conducted to spot out the hydration phases and extent of pozzolanic activity. The incorporation of waste granite dust in AAC conserve river sand resources and also provides sustainable and eco-friendly solution to granite waste dust disposal which otherwise cause environmental degradation and several health hazards.

1.2. Applications of Autoclaved Aerated Concrete

It has numerous applications in construction industry:

- Blocks and precast panels for floors, walls and roofs.
- Load bearing and Non load bearing (architectural).
- Single storey and multi-storey (upto 5 storeys).

1.3. Advantages of Autoclaved Aerated Concrete:

It has numerous advantages over conventional concrete:

a. Light weight
b. Lower Bulk Density
c. Higher Thermal resistivity
d. Lower Shrinkage
e. High Resistance against fire
f. Efficient in construction (Lesser construction time)
g. Energy efficient construction
h. Sound insulation

1.4. Problem Statement

The relatively lower Mechanical properties of AAC limit its use at commercial level, therefore some alternative measures were required to refine the mechanical properties of AAC. High silica mineral in granite waste powder might contribute in pozzolanic activity. Further due to the filler effect of finer particles pore refinement might occurs.

1.5. Research Methodology

The methodology of the study is given in detail as follows:

a. Characterization of Granite powder, Lime and Sand.
b. Selection of Mix design
c. Study the density, water absorption, compressive and flexure strength for each formulation.
d. To have an insight into the response of granite powder's formulations in comparison to the control mix study microstructural properties.
e. Perform thermal conductivity analysis on control and granite powder's formulations
f. Study the response of all formulations against Acid attack

1.6. Research Objectives

Objectives of this study are as follow:

- Characterization of powders(Lime, Granite Powder, Aluminum powder)
- Investigation of Mechanical and Thermal properties of AAC
- Investigation of Durability and Microstructural properties of AAC.

1.7. Scope of Research

Scope of the research is limited to study the influence of granite powder on Mechanical, Thermal and Microstructural properties of Autoclaved Aerated concrete using the aluminum powder as pore forming agent.

CHAPTER 2:LITERATURE REVIEW

2.1. Aerated Concrete

Aerated concrete is a cellular building material which is light in weight. The binder phase in aerated concrete may be cement or lime based mortar. The aeration is done using suitable foaming agent to attain the cellular structure of aerated concrete. There are two types of aerated concrete either it can be non-autoclaved or autoclaved aerated concrete. [18].

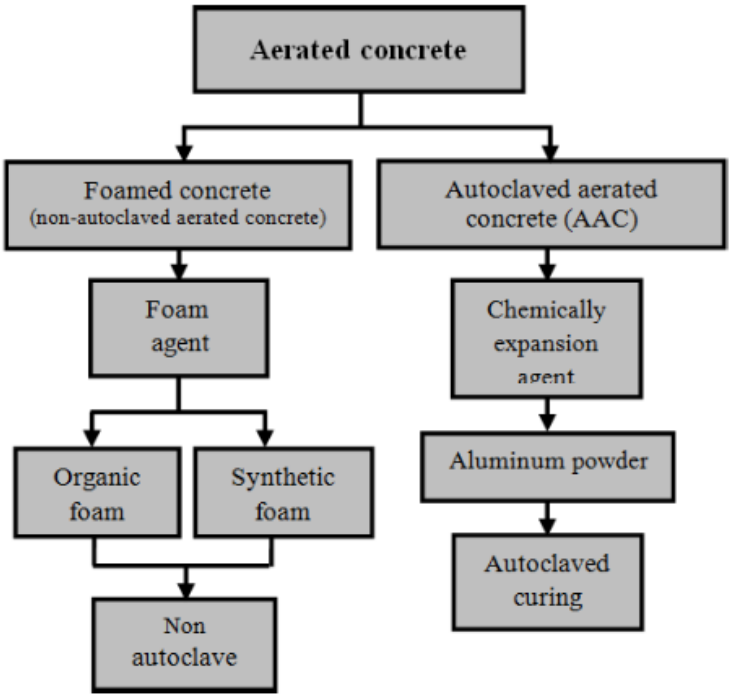

Figure 2. 1: Classification of Aerated Concrete [18]

2.1.1. Foamed Concrete

There are two methods of productions of foam concrete, either by mixed foaming technique or Pre-foaming process. In pre-foaming process the slurry which may be composed of cement paste (cement and water) or cement mortar is prepared separately. To achieve a stable foam the foaming agent is mixed with water and then properly mixed with the separately prepared slurry. In mixed foaming method, both base mix slurry and foaming agent are mixed together and the generation of foam is occur during the mixing of both phases. Based on the manufacturing process the foam is divided into of two categories: wet and dry foam. In case of wet foam the bubble sizes of foam varies from 2mm to 5mm and

the foaming agent is sprinkled on a fine mesh to form a stable foam. Dry foam is usually more stable as compared to the wet foam. In the case the stability of foam is achieved by using foam generator. The size of bubble in case of dry foam is usually less than 1mm which makes it more stable than the wet foam. [18].

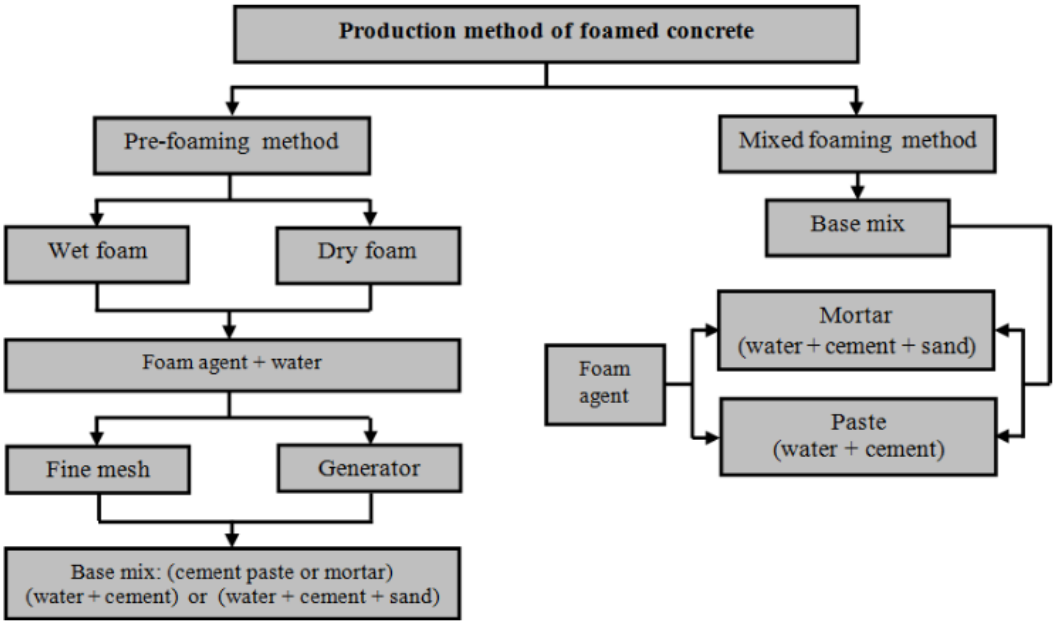

Figure 2. 2: Classification Process of Method for Foam Concrete [18]

2.1.2. Autoclaved Aerated Concrete (AAC)

Autoclave aerated concrete is a type of lightweight concrete containing air voids being generated by the reaction of added aluminum with quick lime and water during cement slurry mixing. It has lower hardened density, shrinkage, comparatively higher thermal resistivity and heat resistance than normal concrete (Dey et al., 2014) (Aroni, 1990) . AAC is eco-friendly building material due to low energy and material consumption during its manufacturing and production phases respectively (Mostafa, 2005). After unmolding the hardened AAC, it is used to be steam cured at elevated temperature between 180 and 200ºC (HFW., 1997.) and pressure of 4-16 MPa for 8-16 hours (Hamad, 2014) to achieve its 28 days strength within first few hours. Generally, AAC is produced from cement, sand, lime as major constituents and aluminum powder as pore forming agent (Kurama et al., 2009). Therefore, aluminum powder reacts with lime and water releasing hydrogen gas bubbles in cement slurry to form aerated concrete (Short A, 1963). A. M. Neville and J. J. Brooks (2010) reported the chemical reaction

occurs between the aluminum powder and lime in presence of water, bubbling off the hydrogen gas in fresh concrete state.

$$2Al + 3Ca(OH)2 + 6H2O \rightarrow 3CaOAl2O3.6H2O + 3H2 \uparrow$$

During autoclaving process, high temperature and pressure alters the chemistry of hydration such as calcium silicate hydrate transforms to crystalline calcium silicate hydrate, therefore, amorphous silica may generate tobermorite crystals on heating, thus to enhance the mechanical properties (H, 2007). Whereas, granite chemically rich in amorphous silica (Asadi Shamsabadi et al., 2018) may increase the concentration of tobermorite crystals due to induced pozzolanic activity of incorporated granite powder in AAC. Ramos et al. (2013) reported that the chemical composition of waste granite powder meets the requirements [(Silica + Alumina + Iron oxide) > 70%] of (ASTM-C618) to be considered as a pozzolanic material.

Aluminum powder has been proved as the best solution for the production of AAC around the globe. Aluminum powder is usually added about 0.2% to 0.5% by dry weight of binder content. In AAC industry Aluminum powder is often manufactured from scrap foils and it occurs in the form of flaky shaped particles. Aluminum powder with particle size less than 50 microns can form dust clouds easily during pouring or vibration, which are highly flammable. The use of aluminum powder with grain size less than 100 or 50 microns produces AAC whose mechanical properties are better.

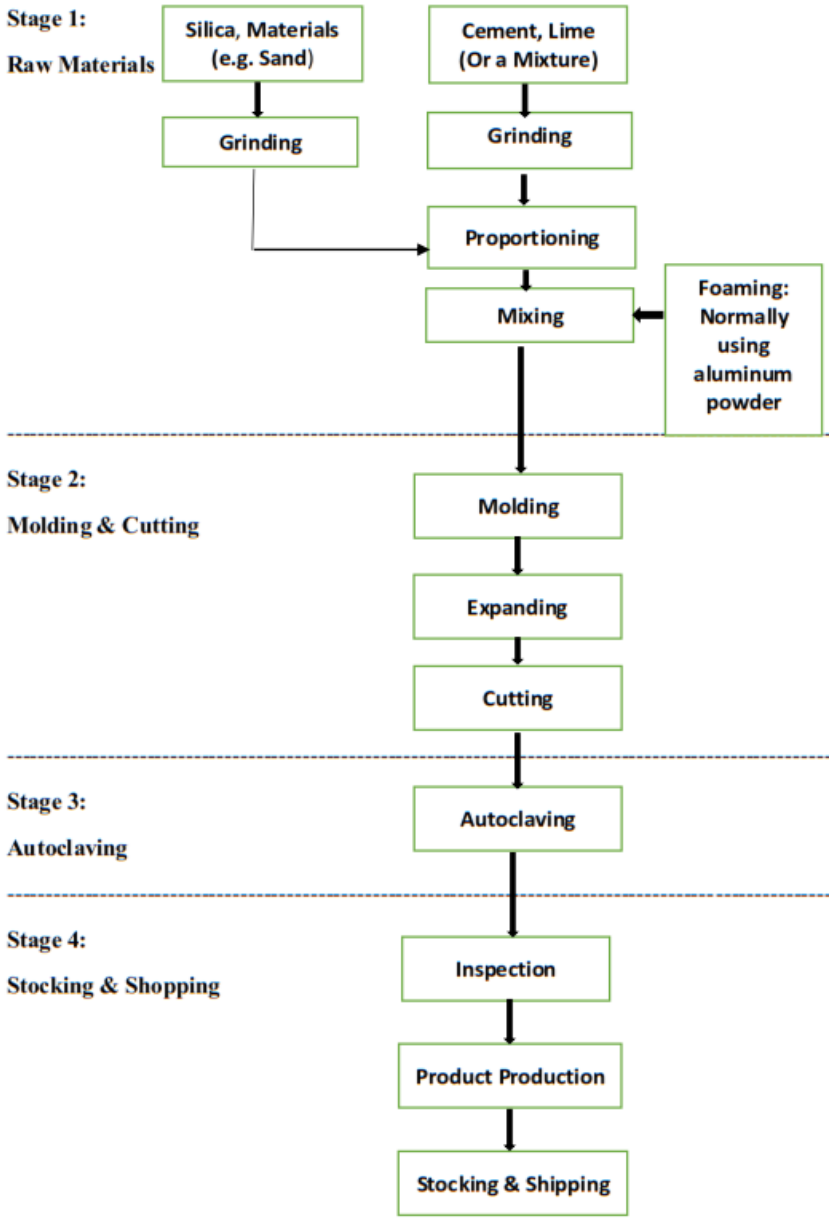

Figure 2. 3: AAC Production Phases [18]

2.2. Classification of Autoclaved Aerated Concrete

Aerated concrete is a cellular building material which is light in weight. The binder phase in aerated concrete may be cement or lime based mortar. The aeration is done using suitable foaming agent to attain the cellular structure of aerated concrete. The properties of this concrete depends on the curing method. There are two methods of curing autoclaved curing and non-autoclaved curing. Based on all these factors aerated concrete can be classified as following:

2.2.1. Based on Aeration Techniques:

2.2.1.1. Air Entraining Agent:

In this aeration technique some kind of air entraining chemicals are added to some extent during the mixing process of aerated concrete. The most commonly used aeration agent is aluminum powder which gives optimum efficiency as compared to other chemicals such as, Hydrogen peroxide, oxygen and acetylene. When aluminum powder is incorporated during mix process its reaction with lime is started in presence of water producing tri-calcium hydrate and hydrogen gas. As the hydrogen gas is lighter than air it will evolved out of mix leaving air bubbles in the mixture. [5].

2.2.1.2. Foaming Agent:

There are two methods of manufacturing foam concrete either by mixed foaming or pre foaming method. This technique is reported as efficient, cost effective and easily manageable to produce light weight concrete [21, 22]. There are further two types of foam based on the nature of material either synthetic based or protein based. There are variety of materials available which can be used for foam generation but glue resins, detergents, resins soap and hydrolyzed proteins are mostly used foaming agents. The air entraining technique with combination of foaming technique can also be used in combination.

2.2.2. Based on Type of Binder

Aerated concrete can be consists of cement mortar, lime mortar or mixture of both. Use of some pozzolanic raw materials are also reported in literature such as coal bottom ash, Rice husk ash and blast furnace slag etc. [13, 23, 24].

2.2.3. Based on Method of Curing

There are two methods of curing it can be either autoclaved or non autoclaved curing. The method and duration of curing significantly influence the properties of aerated concrete such as fresh properties and mechanical properties [5].

2.3. Previous Studies on Autoclaved Aerated Concrete

Previously several research studies have been carried out on AAC. In these studies different properties of AAC were put under consideration by adding some siliceous materials as partial replacement of cement or sand.

Several researchers investigated the mechanical, thermal and durability properties of AAC incorporating agro-industrial wastes as replacement of river sand, such as perlite (Różycka, 2016), coal bottom ash (Wongkeo and Chaipanich, 2010), fly ash (Narayanan, 2000), slag (Mostafa, 2005) and zeolite (Albayrak et al., 2007) as high quartz sand replacement in AAC. Różycka (2016) investigated the physical mechanical, thermal and pozzolanic properties of perlite (sand substituent) added to AAC. Result revealed that 10% perlite substitution yielded desired mechanical and thermal properties with the increased concentration of tobermorite crystals upon added perlite content. Kurama H (2009) incorporated the bottom ash as fine aggregate replacement. The hardened density and thermal conductivity has reduced with increasing the bottom ash percentage whereas, up to 20% addition produced compressive strength results within acceptable limit. Narayanan (2000) investigated the effect of fly ash addition as fine aggregate on microstructure properties of AAC. Results showed the pore refinement evidence because of nucleation sites provided by fly ash particles for hydration products as well as pozzolanic reaction between cementitious phase of fly ash and calcium hydroxide formed as by product of hydration. The replacement of lime and sand by air cooled slag in AAC at several autoclaving times (2, 6, 12 and 24 h) was investigated by Mostafa (2005). The result shown the enhanced microstructural properties at low lime concentration(10%) with the grass like silica rich outgrowth, whereas, at high lime content(30%) lath and needle lie tobermorite crystals appeared. The optimum condition for tobermorite crystals growth observed was 2hours autoclaving time with low incorporated lime content. Albayrak et al. (2007)reported the reduced thermal conductivity of zeolite incorporated AAC with the compressive strength ranged between 1.22-3.34 MPa. Furthermore, Wongkeo and Chaipanich (2010) incorporated the coal bottom ash and silica fume in autoclaved and air cured light weight concrete to study the compressive strength, thermal properties and microstructure. The optimum compressive strength was observed at 20% coal bottom ash with 5% silica fume. Furthermore this incorporation resulted a denser microstructure due to tobermorite formation as compared to the fibrous C-S-H phase detected in control mix.

Various researchers such as Felixkala (2010), Hamza (2011), A. Arivumangai1 (2014), Gupta and Vyas (2018), Sadek (2016), Singh (2016) and Ghannam et al. (2016) have incorporated granite waste as fine aggregate replacement in cement concrete. Felixkala (2010) investigated the incorporation of granite powder as fine aggregate replacement and silica fume, fly ash and slag as cement replacement. Result indicated the enhanced mechanical properties, reduced plastic and drying shrinkage with incremental granite powder content. (Hamza, 2011) investigated the strength and durability properties of concrete bricks incorporating marble and granite powder. Results revealed that the granite powder incorporation increased mechanical and durability properties up to 25% while further incorporation caused the degradation of these properties. Gupta and Vyas (2018) revealed that the granite powder incorporation in cement mortar increase compressive, tensile and adhesive strength. Sadek (2016) stated that high volumes of granite and marble powder might be used as mineral admixtures enhancing strength and durability properties up to 50% replacement of fine aggregates in self-compacting concrete. Singh (2016) utilized the granite cutting waste as a partial replacement of river sand. It was noted that results of compressive strength, abrasion resistance, flexure strength, water absorption, corrosion and carbonation resistance enhanced due to the addition of granite powder waste. Ghannam et al. (2016) investigated the mechanical properties of concrete made with granite powder and iron powder. The compressive strength and flexure strength was increased with addition of granite and iron powder.

The use of granite stone as building material is growing which produce significant amount of waste during its cutting and processing. The amount of waste generated during the processing of granite stone is reported as 50% of the finished granite product volume (Mendoza et al., 2014), (Ramos et al., 2013). In last 10 years the average growth of granite mining and processing industry was approximately 6% of world production per year which makes it the most significant area of mining business (Menezes et al., 2005). Montani (2016) reported that the production of dimension stone in 2015 was 82.6 million tons while the waste generated during processing and extraction was about 70% of total amount. In similar year the production of granite and other siliceous stones is reported historic high of 40 percent. Pakistan has 51 million tons of marble resources in use (Mansoor and Syed, 2012). However, the actual production of granite is quite low due to lack of technological development in this sector, whereas the ratio of waste generated during the mining and processing of granite and marble is quite high in Pakistan.

CHAPTER 3: EXPERIMENTAL PROGRAM

3.1. Materials and Methods

AAC was produced using raw materials including OPC, high quartz sand, waste granite (black) dust, aluminum powder and quick lime. Specific gravity of OPC was found to be 3.15, confirming the requirements of the specification (ASTM C150-04). High quartz sand, collected from river Chenab with fineness modulus value of 1.23, was used as fine aggregate. Waste granite dust (WGD) was used as partial replacement of high quartz sand in AAC. WGD was taken from local marble industry which was produced as a result of cutting, grinding and processing of raw granite. Aluminum powder under brand name of Uni-Chem containing 99% active aluminum was used. Quick lime stone powder, obtained from locally available source, was used after grinding through milling process. Usually, high quartz sand is used in AAC to initiate suitable growth of tobermorite crystals during autoclaving. As WGD was used as sand replacement, the characterization of waste granite dust was conducted to assess its physical as well as chemical contribution towards microstructure enhancement of AAC. The gradation curves of the fine aggregates containing WGD as sand replacement are shown in Fig.3.4. Average particle sizes of grinded lime powder, WGD and aluminum powder were found 1.06, 15.08 and 10.01 microns, respectively, which were determined as per the standard specification of particle analysis size analysis of powders (ASTM E2651-13, 2013), whereas the specific gravity of WGD was found to be 2.45, determined as per (B962-17, 2017). Physical characteristics and chemical composition of cement, lime powder, WGD, sand and aluminum powder are shown in Tables 3.1. It is observed that waste granite powder containing cumulative concentration silica, alumina and iron is 87.41% (>70%) which is one of the chemical requirement of pozzolan as per ASTM C618-17a (2017) whereas it is amorphous. Similar, results were observed for strength and durability properties of granitic quarry sludge waste incorporated mortar (Ramos et al., 2013). Therefore, WGD satisfied both physical (95% passing on sieve no 325 or 45 μm) and chemical requirements (silica+alumina+iron>70%, LOI<6%) to be a pozzolan as per ASTM C618-17a (2017). Morphology and texture of WGD and lime powder were determined by conducting Scanning Electron Microscopy (SEM) as shown in Fig.3.2. Micrograph revealed that WGD is rough, angular and flaky which was also reported by Ramos et al. (2013) and (Ho et al., 2002). Nano-sized WGD particles were seen scattered on micro-sized particles, which might be produced during cutting, grinding and mechanical

polishing of granite, whereas the particle size ranges between 30 µm to 100 nm, as depicted in Fig. 3.2. X-ray diffraction of WGD and quick lime were conducted to assess the mineralogical nature. The X-ray peaks patterns are shown in Fig.3.3. Sharp and highly intense peak of Quartz was identified at 2θ value of 28.22°(d=3.16 Å), whereas comparatively broadened peaks of Wallostonite, Zeolite and Crystobalite were observed at 29.96°(d=2.98 Å), 10.63°(d=8.32 Å), and 22.15°(d=4.01 Å), respectively. As per the published literature, the concentration of component and the intensity of phase diffraction peak are both proportioned to each other, whereas difference in peak phase intensity depicts the concentration difference among the components(Stutzxnan, 1995). The XRD phase diffraction pattern strongly endorsed the abundant presence of amorphous silica in WGD, which is suitable to induce formation of calcium silicate hydrate and tobermorite crystals by pozzolanic reaction (Kunchariyakun et al., 2015). Moreover, morphology and hydration products of WGD and WGD incorporated AAC were examined at microscopic extent by Scanning Electron Microscopy (SEM) using model JSM-5920 JEOL, which will be discussed in the result section.

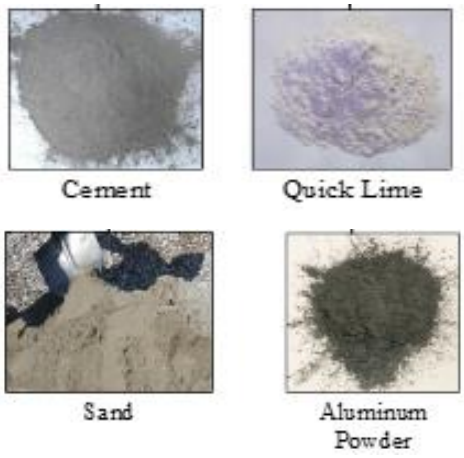

Figure 3. 1: Materials used in AAC

Table 3. 1: Chemical composition and Physical Analysis of OPC, WGD, lime, sand & aluminum powder

Specimen	Purity (%)	Specific gravity	Average particle size (µm)	Specific surface area (m^2/kg)
OPC	-	3.15	16	1100
Waste granite dust	-	2.45	15.08	
Sand	-	2.57	165	-
Quick lime	-	2.32	1.06	1496
Aluminum powder	99.9	-	10.01	-

\\\

Oxide (%)	OPC	Waste granite dust	Quick lime
SiO_2	21.29	65.53	8.49
Al_2O_3	4.82	5.79	-
Fe_2O_3	3.88	16.09	-
CaO	67.12	9.99	91.51
MgO	2.41	-	-
K_2O	0.48	2.60	-
LOI	2.23	1.99	-

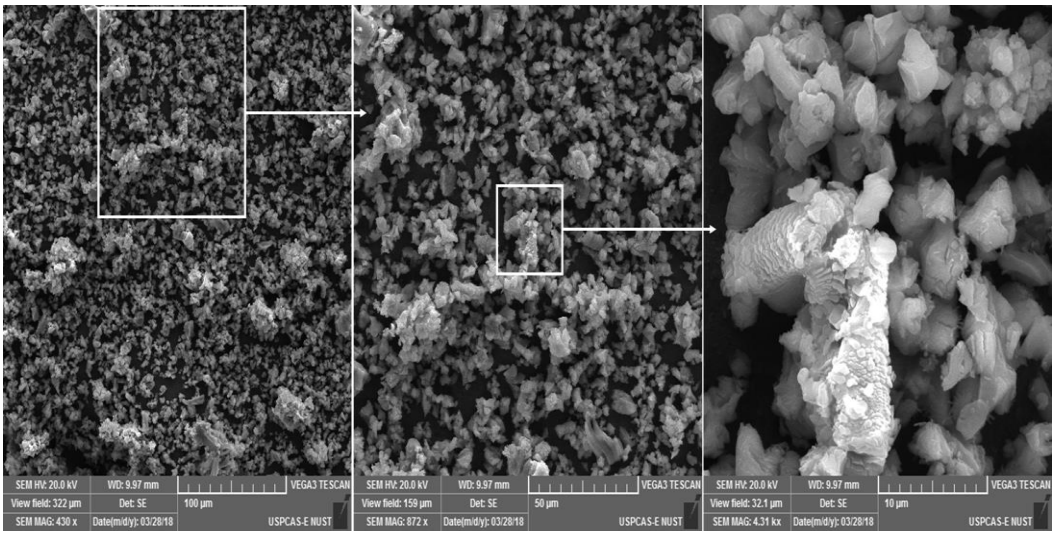

Figure 3. 2: SEM Images of Lime Powder at different magnifications

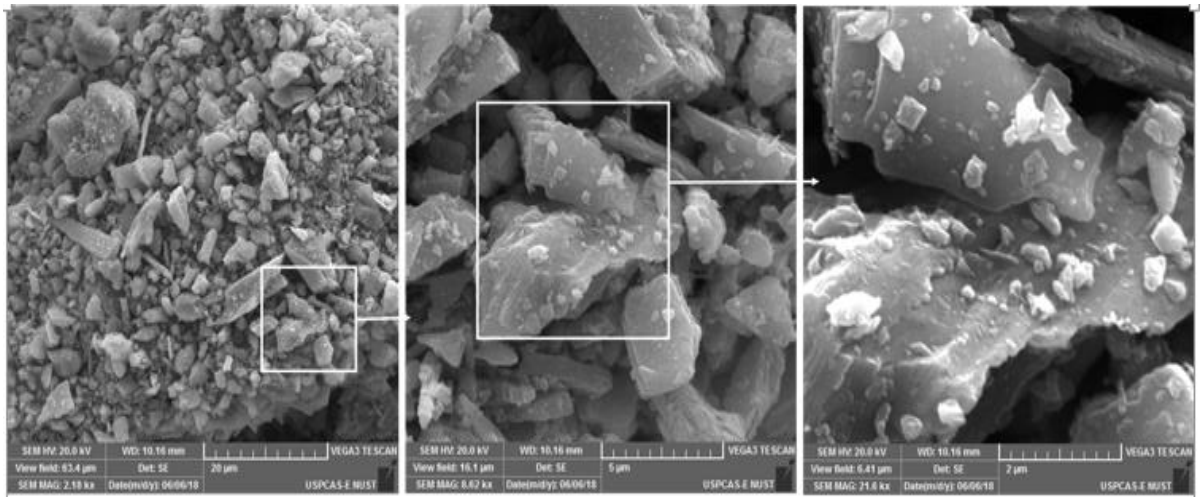

Figure 3. 2: SEM Images of waste granite powder at different magnifications

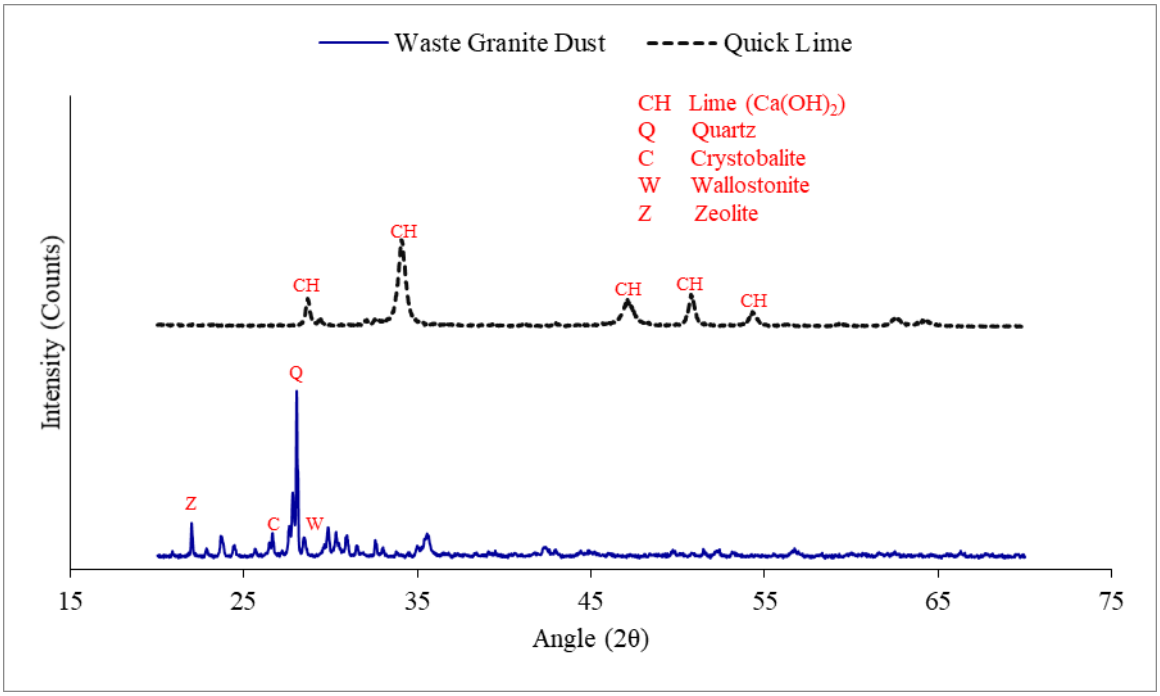

Figure 3. 3: XRD pattern of waste granite dust and quick lime

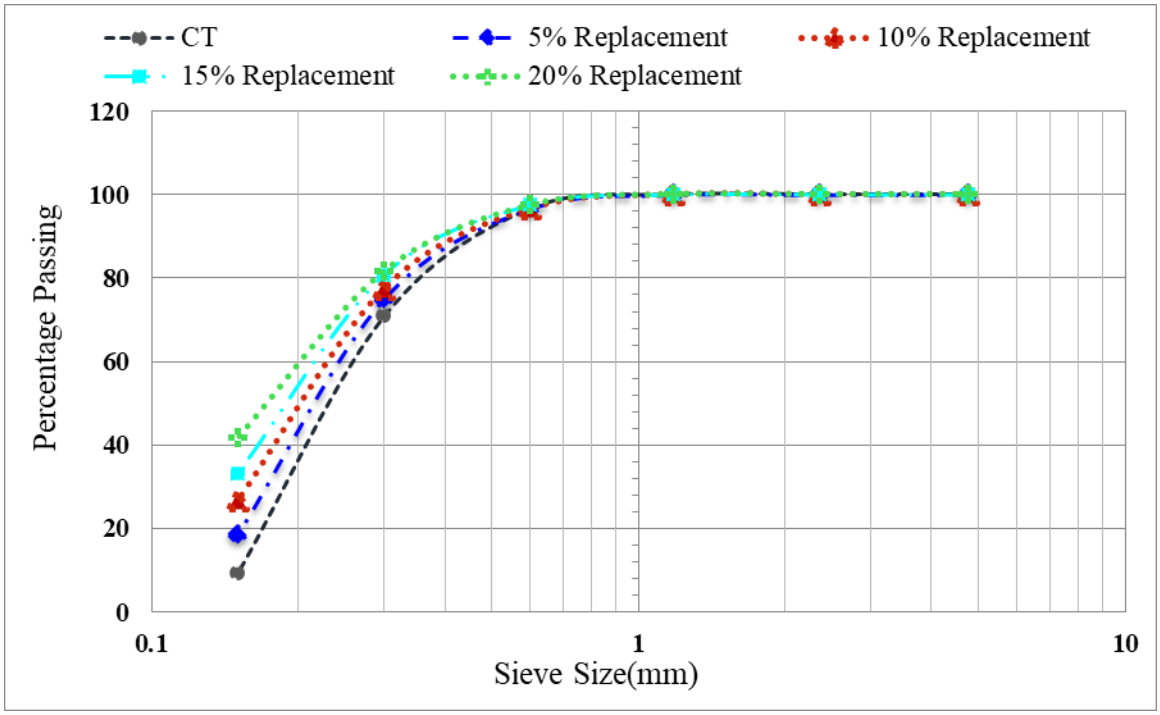

Figure 3. 4: Particle Size Distribution of sand and granite powder composite

3.2. Experimental Program

The research study was carried out in a very organized manner. All the experimental procedures for each and every testing and investigation are described below: the flow chart showing the experimental program is as follows:

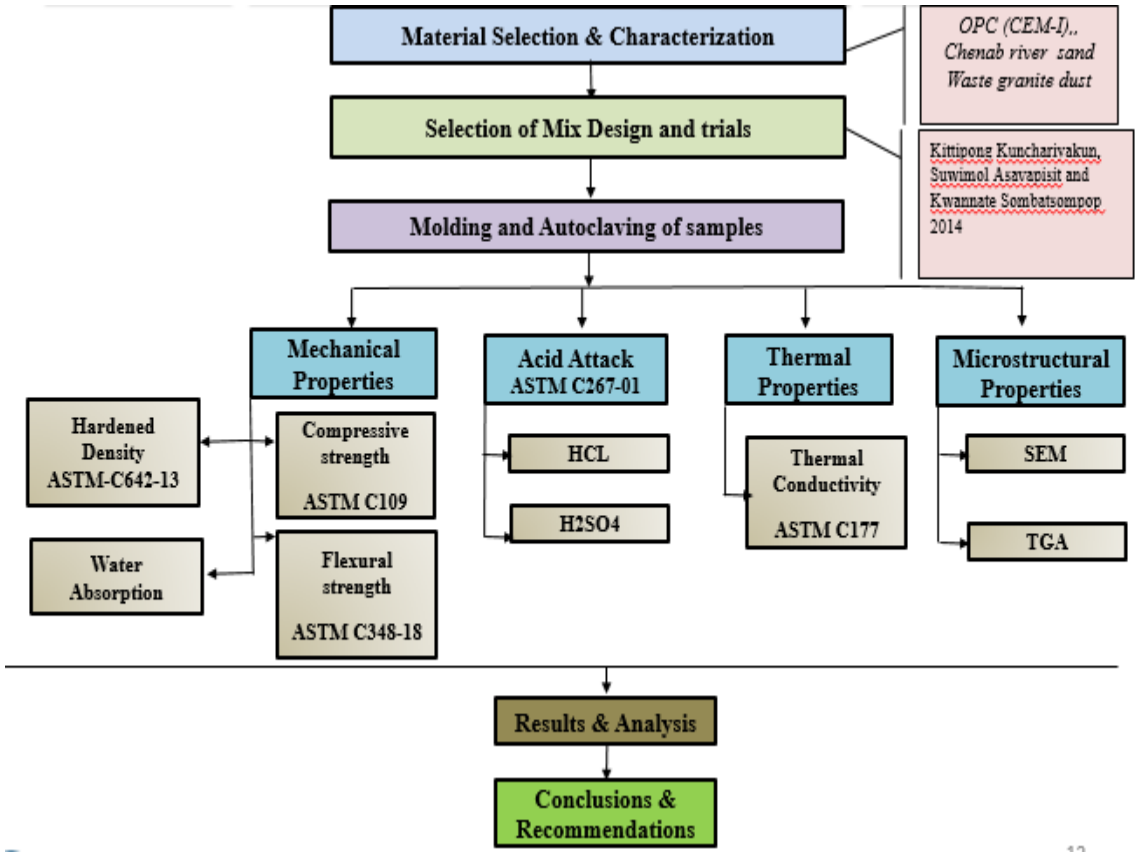

Figure 3. 6: Flow Chart of Experimental Program

All designated autoclave aerated concrete mixes (AAC) were tested for several hardened concrete properties. Although, aluminum powder was used to introduce air bubbles intentionally in all cement slurry mixes. Porosity of AAC specimens was measured by soaking method (water absorption) according to BS1881-122 (2011). During the test, AAC samples were covered with polythene sheet to allow minimal loss of water, whereas sensitivity, relative humidity and temperature were kept as 0.31 microns, 90% and 23± 4.0°C respectively. For hardened concrete properties, density and water absorption were determined as per ASTM C642-13 (2013,), whereas, compressive strength of 5cm mortar cubes was determined as per (ASTM C109 / C109M-02, 2002,). To access the flexural strength of AAC 4 x 4 x 16 cm^3 prisms were casted (ASTM C348-18, 2018,). For both compressive and flexural strength test samples were dried in oven for 24 hours at constant temperature of 40 ^{0}C so that moisture content remains 5% to 15% in samples conforming ASTM C1368-18 (2018,). Thermal conductivity of AAC was assessed in accordance with (ASTM C177-13). Thermo-gravimetric analysis of

AAC was conducted using 10x10mm concrete chunks which were soaked in acetone for stopping hydration just after the autoclaving was completed as mentioned in 'Lea's Chemistry of Cement and Concrete' (Hewlett, 2003). Scanning Electron Microscopy (SEM) aided with Energy Dispersive X-ray Spectroscopy (EDX) of AAC samples was conducted to examine the morphology of AAC, pore sizes and hydration products. The durability of AAC was measured in terms of resistance toward acidic media by immersing the samples in 5% solution of sulphuric and hydrochloric acid separately for 28 days. After removing AAC cubes from acid solutions, cubes were then rinsed in water and oven dried, weight loss and strength loss was recorded afterwards. (ASTM C267-01(2012)) (Thomas et al., 2014)

3.2.1. Mixing Regime and AAC Formulations

Dry mixing of cement, lime, aluminum powder, sand and WGD was employed followed by wet mixing for 1 and 1.5 minutes respectively in Hobart mixer. The fresh cement slurry was poured into 2" cube molds, which afterwards were preheated in electrical oven at 40°C for 3 hours to attain the desired volume stability and setting. After setting of the cement slurry was achieved, the expanded volume of aerated concrete was cut to ensure the dimensional uniformity of the cube. Demolded aerated concrete samples were autoclaved at 180^0C Kunchariyakun et al. (2015) and steam cured at 11 MPa pressure in autoclave chamber for 8 hours (Van Rooyen, 2013), to achieve the 28 days strength within autoclave duration. Conditions of autoclaving process being adopted are similar to the published research (Kunchariyakun et al., 2015). The samples were then tested for physical, mechanical, thermal, durability and microstructural properties. The sequential flowchart of manufacturing process of autoclave aerated concrete is shown in Fig.3.7.

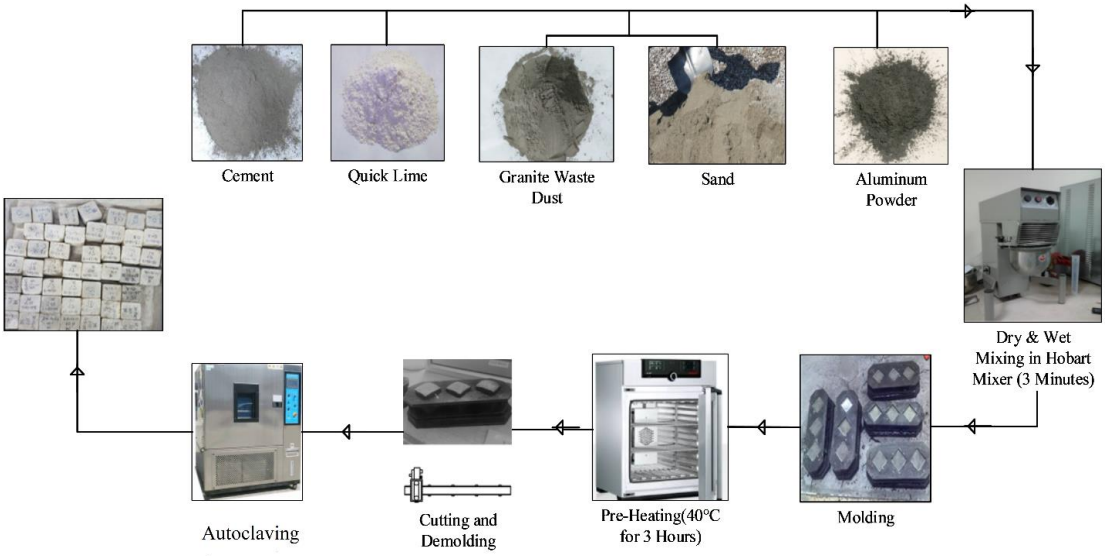

Figure 3. 7: Sequential flowchart for preparation of autoclave aerated concrete

The proportioning of autoclave aerated concrete containing varying percentages of waste granite dust is shown in Table 3.2 Cement and lime contents for all mixes were kept constant at 45% and 5% by weight respectively, whereas 0.5% (weight of binder) aluminum powder was used for aerating fresh cement slurry. High quartz sand was partially replaced with 0, 5, 10, 15, and 20% waste granite dust. Water to binder ratio value was kept constant at 0.65 determined by flow table method in accordance with (ASTM C109 / C109M-02, 2002,)

Table 3. 2: Mix Design of AAC Formulations

Samples	OPC (%)	Cao (%)	Sand (%)	WGD(%)	Al.powder(%)	W/B ratio
CM	45	5	50	-	0.5	0.65
WGD 5%	45	5	45	5	0.5	0.65
WGD 10%	45	5	40	10	0.5	0.65
WGD 15%	45	5	35	15	0.5	0.65
WGD 20%	45	5	30	20	0.5	0.65

3.2.2. Strength Tests

For compressive strength test, the dimensions of the specimens were 5x5x5 cm^3. While for flexure strength test, prism of 4x4x16 cm^3 were cast. Three specimens were tested according to BS EN standards for each formulation and average results were reported. For determining compressive and flexure strength of each formulation at 5 hour of accelerated curing, specimens were tested in the direction of their rise in compression testing machine according to ASTM C1368 standards as shown in Fig.3.8.

Figure 3. 5: Compression testing machine

3.2.3. Water Absorption Test

Water absorption capacities of all the AAC mixes were determined according to ASTM C642-97. The test was performed on the 5 cm x 5 cm x 5cm cubes. After 5 hours of steam curing, cubes were taken out of water and oven dried at of 100±5 °C for 24 hours. Then cubes were taken out of the oven and weighed in dry conditions. Then cubes were kept in water for 24 hours and weighed in SSD conditions. The Difference of two weights for each cube gave the moisture content absorbed by the respective formulation.

3.2.4. Scanning Electron Microscopy

To investigate the particle size, shape and morphology of Lime Powder and Granite powder and also to study the hydration products, microstructure and ITZ of AAC formulations, scanning electron microscopy was carried. Broken pieces of AAC mixes

were collected and oven dried at 100±5 °C for 24 h to stop the hydration process and make the samples free from moisture. Then samples were broken into required size and stuck with carbon tape on studs to obtain clear and more perceivable images. Then gold coating was done using sputter coater. SEM analysis was performed using model "TESCAN VEGA3".

3.2.5. Energy Dispersive X-Ray (EDX) Analysis

To verify the formation of tobermorite crystals in AAC formulations containing dosage of granite powder EDX spot analysis were performed on each of the three specimens considered for SEM using the model "TESCAN VEGA3" Scanning electron microscope equipment to study the chemical composition.

3.2.6. Resistance to Acid Attack

For determining the resistance to acid attack, three cubes (5cm x 5cm x 5cm) samples of each formulation were casted. After pouring the slurry of mixes in to the moulds, preheating was carried out for 3 hours at a temperature of 40 °C. Then steam curing was carried out for 5 hours at a temperature of 140 °C. After curing samples were taken out and dried in oven for 24 hours at a temperature of 100±5 °C and dry weights were recorded. Now the samples were immersed in 5% solution of hydrochloric and sulfuric acids for 28 days. After 28 days samples were again dried in oven for 24 hours. Percentage weight loss was determined from these recorded weights. This test was carried out to check the durability of AAC mixes.

3.2.7. Thermogravimetric Analysis (TGA)

Thermogravimetric analysis of AAC mixes was done to explore the possible Pozzolanic potential of granite powder. Thermogravimetric analysis was performed on CT, WGD10 and WGD20 mixes. Qualitative analysis was carried out on specimens of AAC mixes after steam curing of 8 hours at a temperature of 180 °C. Samples were kept in controlled furnace and Nitrogen gas was used as atmosphere at a rate of 50 ml/min in the furnace. Starting temperature was kept 28 °C for 2 minutes and then temperature was increased upto 900 °C at a controlled rate of 10 °C/min. The weight loss was logged corresponding to the temperature of samples during the disclosure time.

3.2.8. Thermal Conductivity

To investigate the durability and insulation properties of three specimens used in SEM and EDX analysis, Thermal conductivity tests were performed on AAC samples with surface area 50mm x 50mm at NED University of Engineering and Technology Karachi.

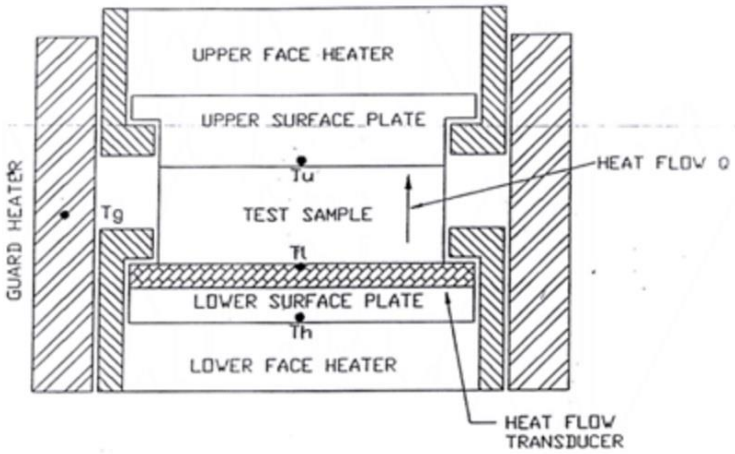

Figure 3. 6: Guarded heat flow meter apparatus [ASTM 1530-11]

Thermal conductivity describes the insulation properties whereas electrical resistivity is a measure to quantify the ability to resist corrosion or durability of cementitious systems. Thermal conductivity tests were performed following ASTM E1530-11 Standards, using guarded heat flow meter apparatus as shown in Figure 3.10.

CHAPTER 4:RESULTS AND DISCUSSION

4.2. Compressive Strength of AAC

The compressive strength results of AAC containing granite powder as fine aggregate replacement is shown in figure 4.1. The Compressive strength of AAC at different incorporation percentages of WGD was observed to increase till WGD20 mix. The maximum increase in compressive strength was recorded as 42% at WGD20 mix comparative to CM mix. Therefore, highest compressive strength of WGD20 mix corresponded as optimum one. The increasing trend of compressive strength is due to the pozzolanic activity by consumption of hexagonal crystals of portlandite and growth of densely packed C-S-H gel and tobermorite crystals being evident from SEM analysis (Fig.7). Similar trends of mechanical and microstructural properties were observed by Różycka et al. (Różycka, 2016), in which perlite waste addition enhanced the microstructure by the formation of calcium silicate hydrate gel. Kurama et al. (Kurama H, 2009) reported that the incorporation of coal bottom ash in AAC has increased compressive strength up to 50% replacement level.

A linear trend line co-relation between hardened density and compressive strength inclining upward with the regression equation and coefficient value of “density = 44.079(comp. strength) + 872.39” and 0.98, respectively, indicating good correlation between data points and linear curve being plotted as shown in Fig.4.2. Narayanan et al. (Narayanan, N and Ramamurthy, K, 2000) reported the proportionate correlation between density and compressive strength of AAC.

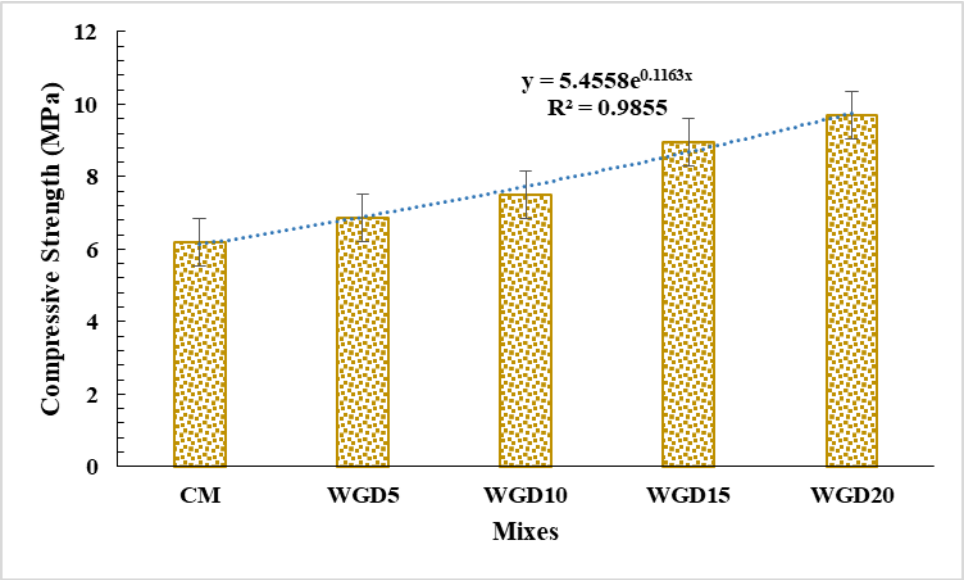

Figure 4. 1: Compressive strength of AAC mixes

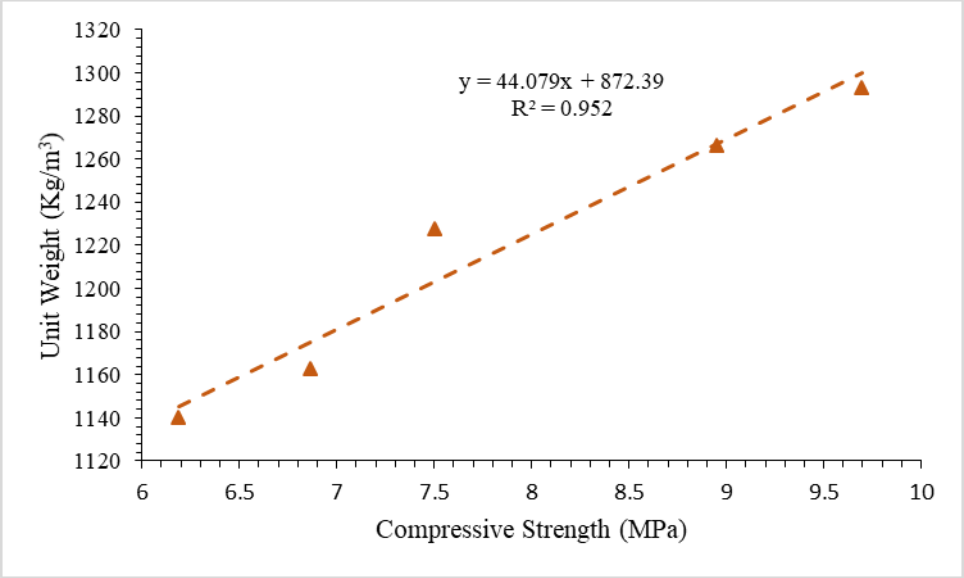

Figure 4. 2: Relationship between compressive strength and density of AAC

4.3. Flexure Strength of AAC

Flexure strength and relationship between flexure strength and dry densities of AAC formulations obtained are shown in Fig. 4.3 and Fig. 4.4 respectively. The trends of flexure strength results are similar to those of physical(such as density) and mechanical properties as reported in literature (Schober, 2005). The flexure strength increased along

replacement of incorporated WGD content. The flexure strength for different AAC samples ranged between 0.42 and 0.58 MPa with the trend line regression equation and coefficient are "flexure strength = $0.3916e^{0.0806WGD}$" and 0.98 respectively. It is evident in Fig.4.4 that both the flexure and compressive strengths have direct relationship. In addition, exponential regression equation is plotted for AAC formulation from which the trend of flexure strength with increase in waste granite dust can be interpolated. The correlation regression equation and coefficient are "flexure strength = $0.2553e^{0.0854(comp.\ strength)}$" and 0.98 respectively, higher value of correlation coefficient depicted the excellent relation between data points and regression curve.

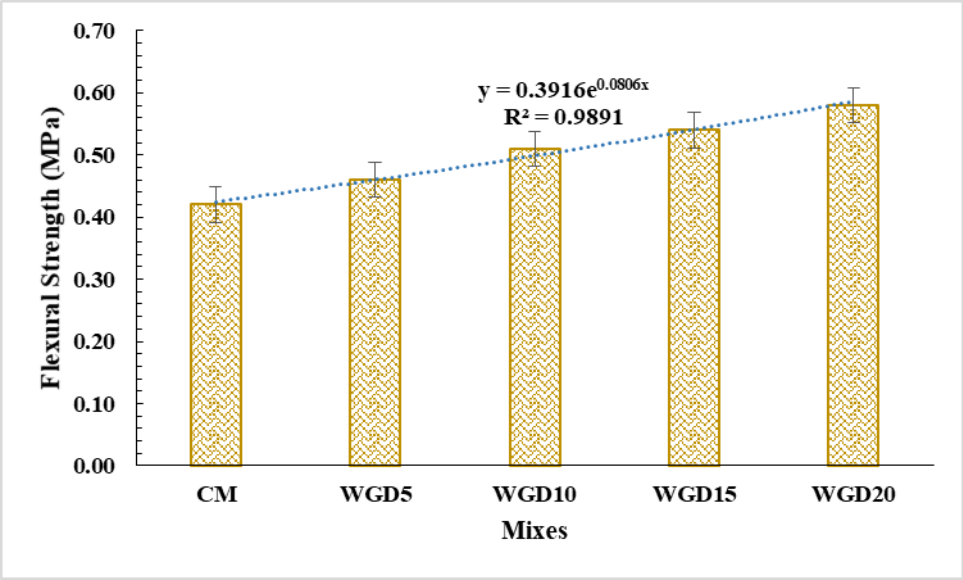

Figure 4. 3: Flexure strength of AAC mixes

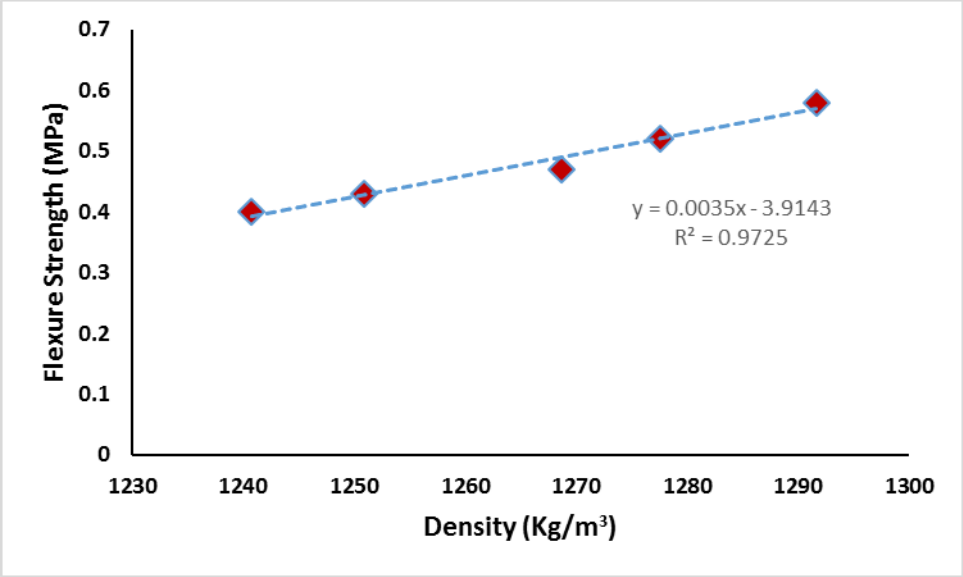

Figure 4. 4: Relationship between flexure strength and density of AAC

4.4. Unit Weight and Water Absorption of AAC

The dry densities of AAC samples cured for 8h are illustrated in figure 4.7. The hardened density depicts quality and classify the use of AAC. The hardened density of AAC lies in the range of 400 Kg/m^3 to 1600 Kg/m^3 (Newman & Choo, 2003). The maximum and minimum densities observed was 1139.93 and 1293.32 Kg/m^3 for GP20 and CM mixes respectively. Total increase of 13.45% in hardened density oberved between CM and GP20 mixes along the regression equation and coefficient values of "hardened density = $1099.2e^{0.0338WGD}$" and $R^2 = 0.97$ respectively. The densification of cement paste matrix by pore micro-filling is evident in published literature (Siddique, 2003)), whereas the increasing values of hardened density upon addition of WGD in AAC is due to filling of air voids by nano and micro sized waste granite dust particles. Siddique et al. ((R. Siddique, 2011) observed that the addition of foundry sand caused the hexagonal calcium hydroxide crystals to disappear due to consumption in concrete. However, the incremental addition of WGD in AAC replaced the low density portlandite into higher density tobermorite crystals. Conclusively, the increasing trend of hardened density upon WGD addition was due to physical filling of voids by nano and micro sized WGD particles and densification of AAC microstructure by transformation of lower density $Ca(OH)_2$ into higher density tobermorite crystals as evidenced in microstructure analysis of AAC being discussed.

The relationship between density and water absorption is also shown in figure 4.5. Water absorption capacity or permeability is significantly reduced for AAC containing granite powder as compared to control mix. The reduction in water absorption is related to the dense microstructure of AAC with granite powder replacement. It is due to the close packing of hydration products which is due to the outgrowth of tobermorite crystals bridging the pores as visible in SEM micrographs in Fig. 4.10.

The results of water absorption indicated that the water absorption of AAC reduced along all added WGD replacements with the minimum value detected at GP20 mix due to discontinuity of connected pores by densification of microstructure as a result of tobermorite formation and nano-micro filling of voids, similar behavior was recorded by Singh et al. (Singh, 2016) in high strength concrete containing granite cutting waste. The exponential regression equation of all mixes for water absorption came out as water absorption = $26.856e^{-0.001xWGD}$ with the regression coefficient R=0.96.

The co-relation between hardened density and water absorption being plotted parallel in ordinate with the values of WGD percentage addition on abscissa as shown in Fig 4.5. The polynomial trend line equation for both hardened density and water absorption with regression coefficients values of 0.9742 and 0.9616 respectively, indicated the strong relation between data points and plotted curves. The co-relation curves are inversely proportion to each other, however water absorption decreased with the increase of hardened density along the varying percentages of WGD in AAC. The curves coincide with each other between GP05 and GP20 mixes at the point of intersection projected on abscissa value of around 8% WGD content with the hardened density value of 1210 Kg/m^3. The maximum hardened density and minimum water absorption was observed at GP20, while minimum hardened density and maximum water absorption was recorded for the CM mix. This trending behavior of hardened density and water absorption co-relation curves being observed might due to the enhanced microstructural properties through densification of cement paste matrix due to consumption and growth of lower density portlandite and C-S-H gel respectively as a result of pozzolanic reaction along micro-nano filling of GWD. Singh et al. (Singh, 2016) and Siddique et. al. (R. Siddique, 2011) reported the similar trend of concrete density upon granite cutting waste and foundry sand addition respectively.

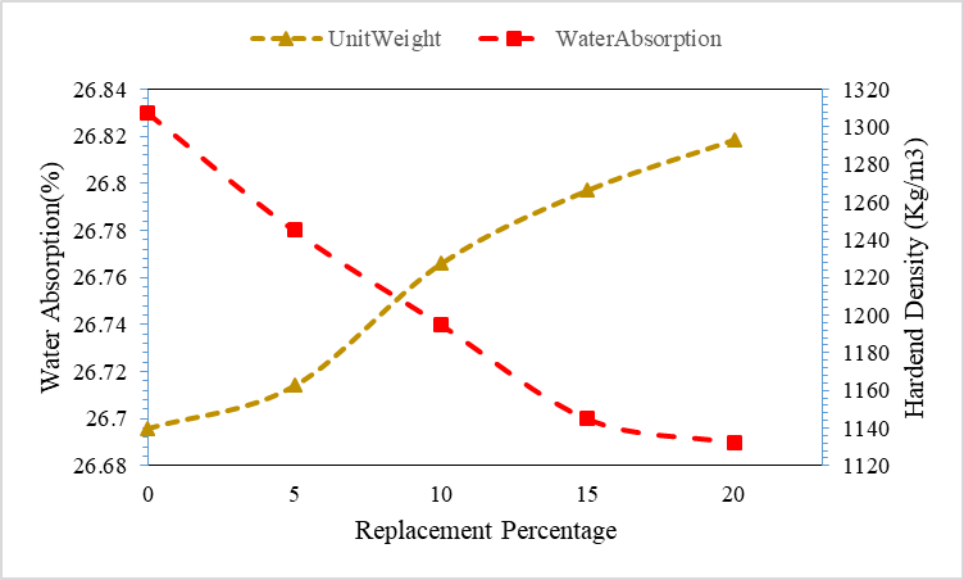

Figure 4. 5: Relationship between the water absorption and density

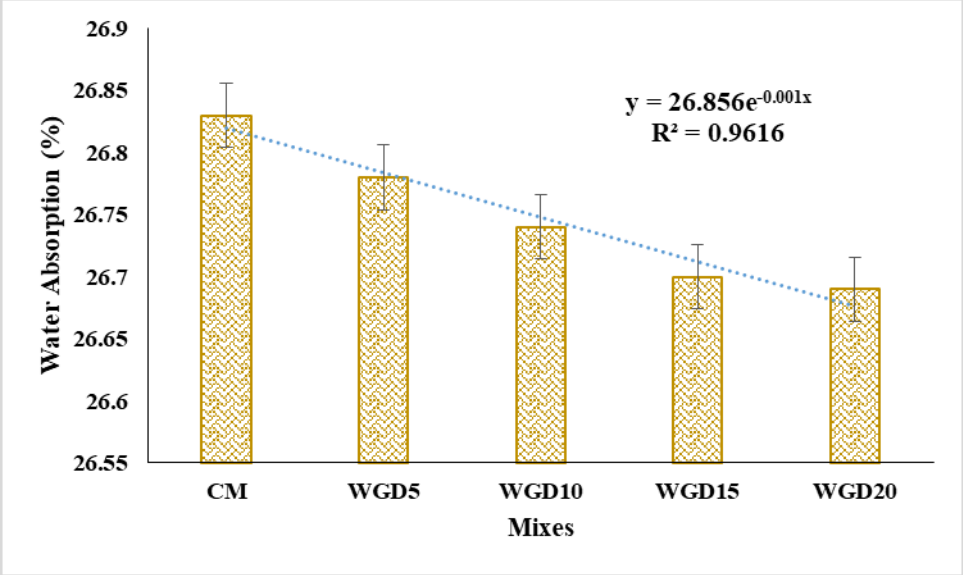

Figure 4. 6: Water absorption of AAC mixes

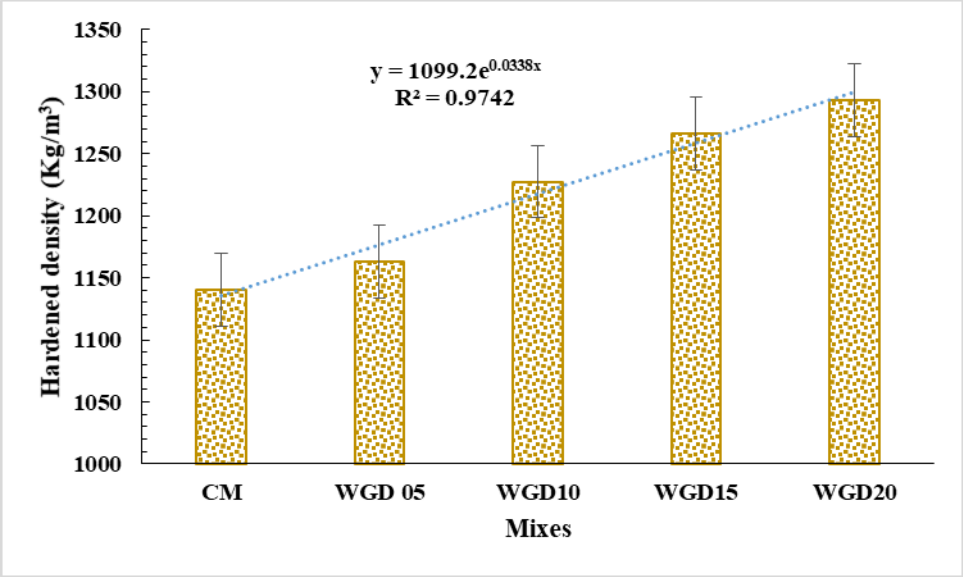

Figure 4. 7: Hardened density of AAC mixes

4.6. Acid Attack

The results indicated that the weight loss and strength loss of AAC for sulphuric acid were found considerably higher than that of hydrochloric acid. In case of hydrochloric acid, higher weight loss and strength loss attributed to the expensive natured Delayed Ettringite Formation(DEF) which deteriorate concrete by cracking and spalling for further ingress of acid into concrete matrix (P. Kumar Mehta, 2006). When sulfuric acid penetrate into the concrete mixes its reaction with calcium hydroxide which is present in cement hydrates will result the formation of gypsum due to which the hydration products will expand causing the erosion (Kawai, Yamaji, & Shinmi, 2005).

$$H_2SO_4 + Ca(OH)_2 \longrightarrow Ca(SO)_4 + 2H_2O$$

Acid + Calcium Hydroxide $\longrightarrow$ Calcium Sulfate+ Water

($Ca(SO)_4$ results sulfate attack)

For HCL, weight loss recorded was 3.85 and 1.33% for GP0 and GP20 respectively. Weight loss of H2SO4 recorded were 5.45 and 3.25% respectively. Decreasing trend in weight loss indicated the enhancement of microstructure by filler effect and pozzolanic activity.

$$2HCl + Ca(OH)_2 \longrightarrow CaCl_2 + 2H_2O$$

Sulfuric acid is more aggressive in nature as compared to hydrochloric acid which is the reason that the weight and strength loss of AAC against sulfuric acid is more than hydrochloric acid.

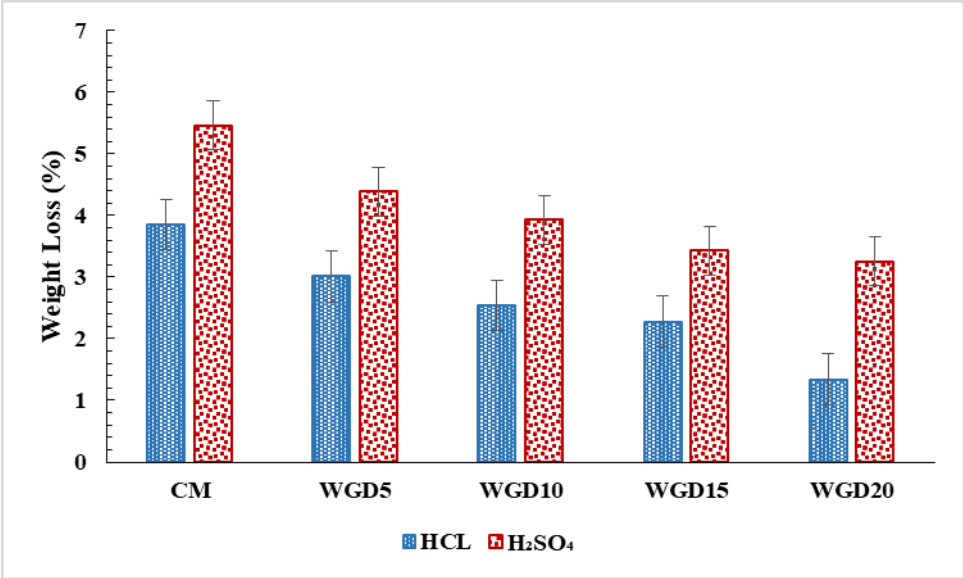

Figure 4. 8: Weight loss % of AAC mixes

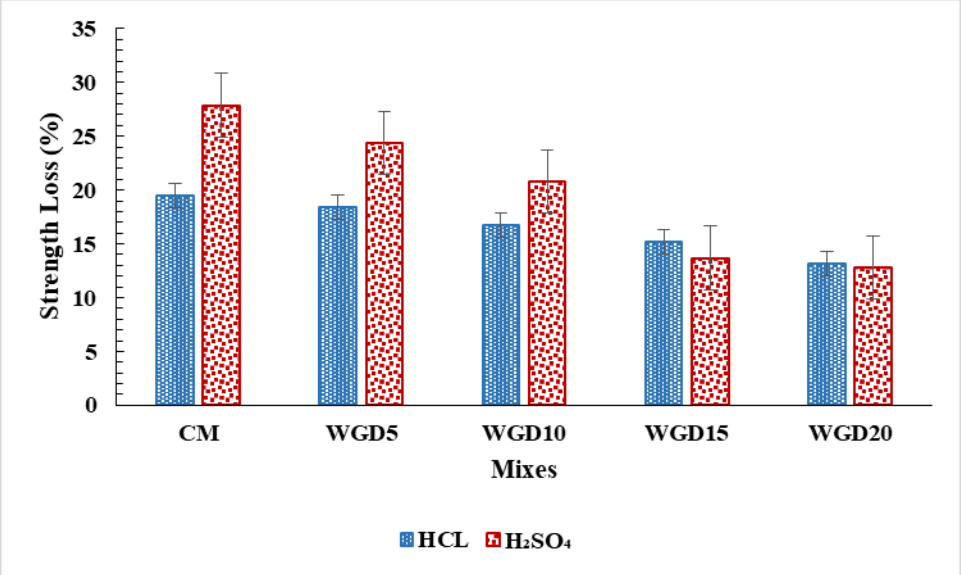

Figure 4. 9: Strength loss % of AAC mixes

4.7. Scanning Electron Microscopy of AAC

Scanning Electron Microscopy (SEM) showed the surface morphology and hydration products in WGD incorporated AAC samples for CM, GP10 and GP20 is shown in Fig. 4.10. The wider pore sizes observed between 50-200µm for CM mix in Fig.4.10 (a), which were reduced to around 5 and 3 micron for GP10 and GP20 respectively. Surface texture and morphology of AAC improved by gradual inclusion of WGD due to pore filling and refinement by physical filling of WGD, with the particle size ranged between 100nm and 30µm. The SEM micrographs illustrated the formation of needle like tobermorite crystals being surrounded the hexagonal crystals of calcium hydroxide in control mix (Fig. 4.10a) which were further transformed into grass like, fibrous but density interconnected tobermorite crystals in GP10 mix, whereas transformation of $Ca(OH)_2$ into fibrous C-S-H gel has been observed in GP20 mix (Fig.4.10b). Moreover the maturity of tobermorite crystals is evident in GP20 mix comparative to CM and GP10 mixes, which resulted densified microstructure. The hexagonal $Ca(OH)_2$ crystals were abundantly occupied the space in CM mix, which were consumed during pozzolanic reaction between amorphous silica present in WGD and calcium hydroxide. Energy Dispersive X-ray spectroscopy (EDX) on similar SEM micrographs was conducted for identifying hydration phases in AAC, which are shown in Fig. 4.11, while calcium silica ratios (Ca/Si) are presented in Table 4.1.

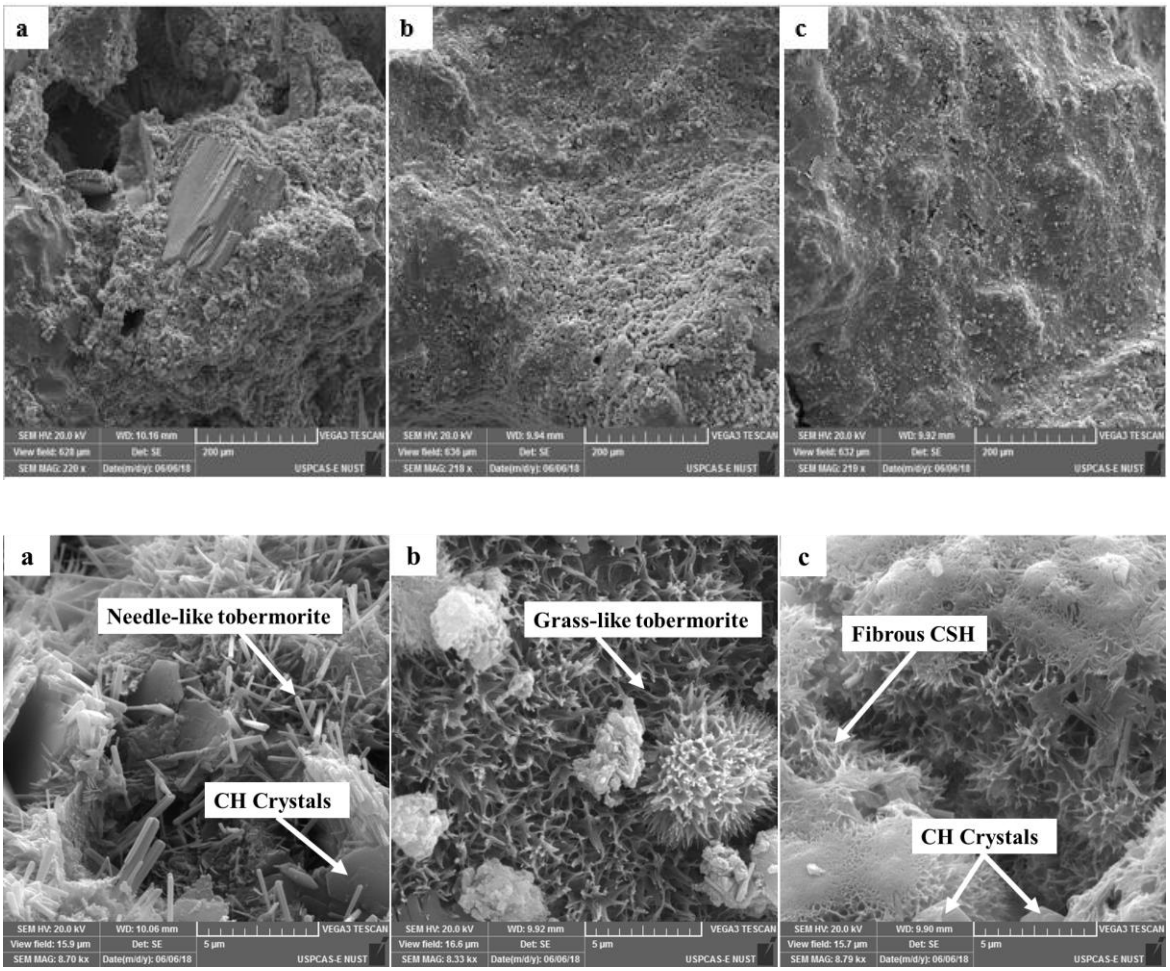

Figure 4. 10: SEM micrographs of Control mix (a),WGD20 (b) and WGD10 (c)

From the literature it is evident that Ca/Si ratio of the initiating materials affect the morphology of tobermorite crystals (Mostafa, 2005), (Hong & Glasser, 2004) (Mostafa, El-Hemaly, Al-Wakeel, El-Korashy, & Brown, 2001), (Mostafa, 1995), (Mitsuda, Toraya, Okada, & Shimoda, 1988). Ca/Si ratio plays a pivotal role in determining the crystalline phase evolution (K. Kunchariyakun, Asavapisit, & Sinyoung, 2018; K. Kunchariyakun, Asavapisit, S., & Sombatsompop, K., 2015). When the sand is replaced with highly reactive siliceous based material (such as waste granite dust) in finely ground form, a declination in Ca/Si ratio occurred because of the presence of less reactive and inert silica in quartz sand. At higher Ca/Si ratios (>1), first needle shaped tobermorite crystals were formed, while at lower Ca/Si ratio (<1), caused the formation of plate like and crumbled foil like tobermorite crystals (K. Kunchariyakun et al., 2018), (K. Kunchariyakun et al., 2015). However, plate like/crumble foiled tobermorite crystals shown prominently shown in figure 4.10-c for GP10 mix with Ca/Si ratio value of 0.99. Furthermore, it can be deduced that concentration of tobermorite increased upon

incremental addition of WGD. Previous literature also reported that the optimum range of Ca/Si ratio for the formation of tobermorite crystals lies between (0.8-1.0) (K. Kunchariyakun et al., 2015), (Mostafa, 2005). Fibrous C-S-H with Ca/Si ratio below 0.8 hardly transformed to tobermorite crystals. Their transformation is prohibited and rate of transformation is very slow. While the CSH with Grass like structure having Ca/Si ratio greater than 1.0 can easily be transformed to tobermorite crystals because of the tendency to have short chained silica at early stages (HFW., 1997.), (Cong & Kirkpatrick, 1996), (Sato & Grutzeck, 1991). In this research, the energy dispersive spectroscopy (EDS) of AAC illustrated that the Ca/Si ratios of the crystalline phases were 1.40, 0.99 and 0.94 for Control mix, GP10 mix and GP20 mix respectively, which showed the positive indication of densification of microstructure by plate like tobermorite formation by consumption of calcium hydroxide crystals in WGD added autoclave aerated concrete matrix. Conclusively, microstructure of AAC being enhanced by physical filler effect of WGD, maturity of tobermorite crystals and transformation of hexagonal calcium hydroxide crystals into C-S-H gel being evidenced from calcium silica ratios of the mixes.

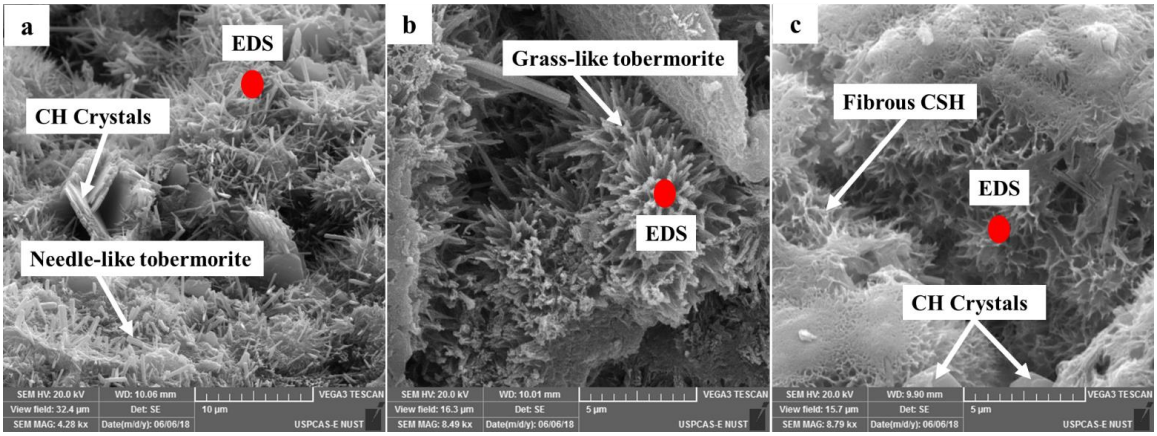

Figure 4.11: SEM micrographs of AAC showing EDS spots (a) Control (b) GP20 and (c) GP10

Table 4.1 Atomic Weights of AAC Samples

Elements		Percentage Atomic Weight	
	CT	**GP10**	**GP20**
C	24.47	23.95	25.78
O	61.30	61.91	59.71
Mg	0.60	0.20	0.10
Al	0.59	0.51	0.46
Si	5.25	6.58	7.98
K	0.26	0.13	0.19
Ca	7.37	6.57	7.57
Fe	0.16	0.15	0.17
Ca/Si ratio	**1.40**	**0.99**	**0.94**
Ca/(Si+Al)	**1.26**	**0.92**	**0.89**
Al/(Si+Al)	**0.101**	**0.04**	**0.02**

4.8. Thermogravimetric Analysis

Thermogravimetric analysis (TGA) of AAC samples was employed to assess the pozzolanic potential of WGD being incorporated in autoclave aerated concrete. For quantitative analysis, TGA of CM, WGD10 and WGD20 mixes was performed after the fresh samples were accelerated cured at temperature and pressure of 180°C±5 and 11 MPa, respectively. The weight loss values for CM, WGD10 and WGD20 mixes are shown in Fig.4.12 and Table 4.2. Three weight loss regions were detected based on chemical dissociation of minerals at certain temperature, as endorsed by the literature (Xu, 2015). The first weight loss region between temperature range of 110-300°C depicts the loss of physically attached and chemically bonded water from CSH gel. The temperature range for second weight loss region was recorded between 400-600°C due to dehydroxylation of portlandite $Ca(OH)_2$. Furthermore, calcium carbonate decarbonated within the temperature range of 750-900°C (Xu et al., 2015). From the Fig.4.12, the weight loss of control mix, WGD10 and WGD20, in first region was calculated to be 4.10, 3.43 and 3.62% respectively. The minimum of portlandite dissociation for WGD20 (3.53%) was observed in second weight loss region as compared to the control mix and WGD10 mix with the values of 3.66 and 3.54, respectively. The lowest representation of portlandite shows the extent of pozzolanic activities in AAC, due to consumption of portlandite in pozzolanic reaction with amorphous silica in WGD. It is evident from the

results that the granite powder enhances the strength development rate and improves the microstructure by replacing low density portlandite with higher density secondary C-S-H gel. Therefore, the pozzolanic potential of granite dust incorporated in AAC as fine aggregate is justified.

Table 4.2: Weight loss of AAC mixes

Mixes	Weight loss (%)		
	Stage 1	Stage 2	Stage 3
CM	4.10	3.66	0.59
WGD10	3.43	3.54	0.68
WGD20	3.62	3.53	0.77

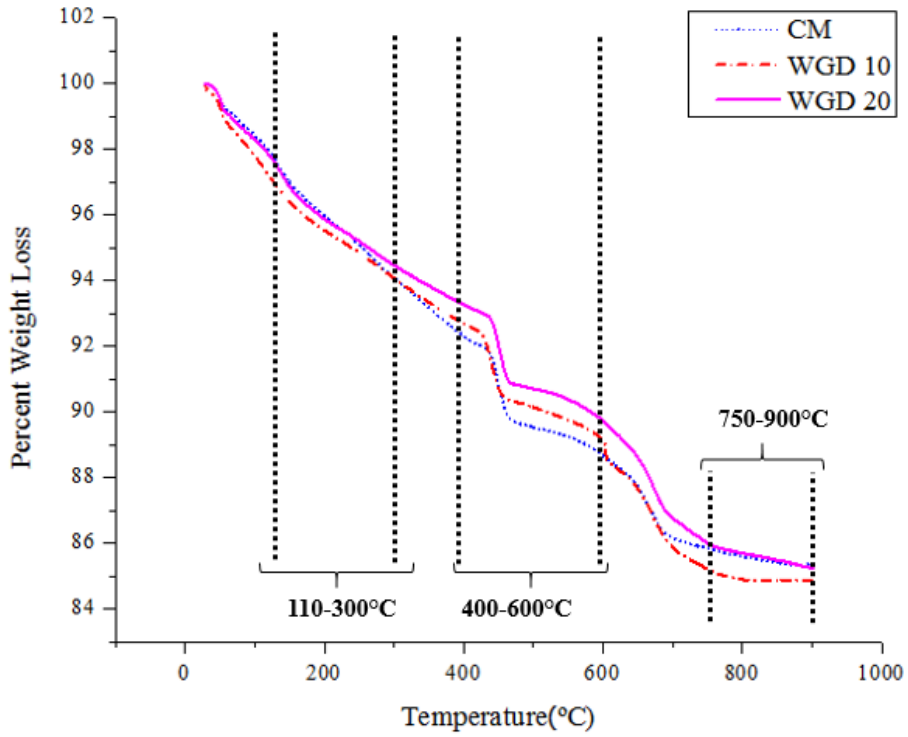

Figure 4. 12: TGA results of AAC mixes

4.9: Thermal Conductivity

Thermal conductivity results of Autoclaved aerated concrete containing control and WGD mixes are shown in figure 4.13. As thermal conductivity is a function of density and microstructure, therefore, increasing thermal conductivity values from CM to WGD20 mixes depict the densification of microstructure by enhanced tobermorite crystals formation in AAC microstructure (Fig.4.10). Thermal conductivity values of CM, WGD10 and WGD20 mixes were found to be 0.245, 0.275, 0.332 W/mK, respectively. Thermal conductivity depends upon the pore size distribution, connectivity and moisture content (A Bonakdar, 2013; Narayanan and Ramamurthy, 2000). Therefore, all of the thermal conductivity influencing parameters supported it to increase the conductivity values along WGD replacement because of the pore size, connectivity and distribution being reduced by clogging effect due to the dispersion of WGD and increased pozzolanic products concentration in cement paste matrix. It can be interpreted from the results that waste granite dust addition increases thermal conductivity optimally up to WGD20 mix due to the enhanced microstructure.

Linear correlation can be observed between hardened density and compressive strength placed parallel on ordinate, whereas thermal conductivity on abscissa as shown in Fig.4.14. In other words, hardened density increased with considerably greater rate than the compressive strength at fixed thermal conductivity values. Conclusively, thermal conductivity exhibits a direct relation with compressive strength and hardened density, whereas slower rate of strength gain along replacement content of WGD was attributed only to the chemical gelling effect of tobermorite crystals and CSH growth in cement matrix. On the other hand, hardened density increased with higher rate due to both chemical effect (pozzolanic reaction) and physical effect (clogging and micro-filling).

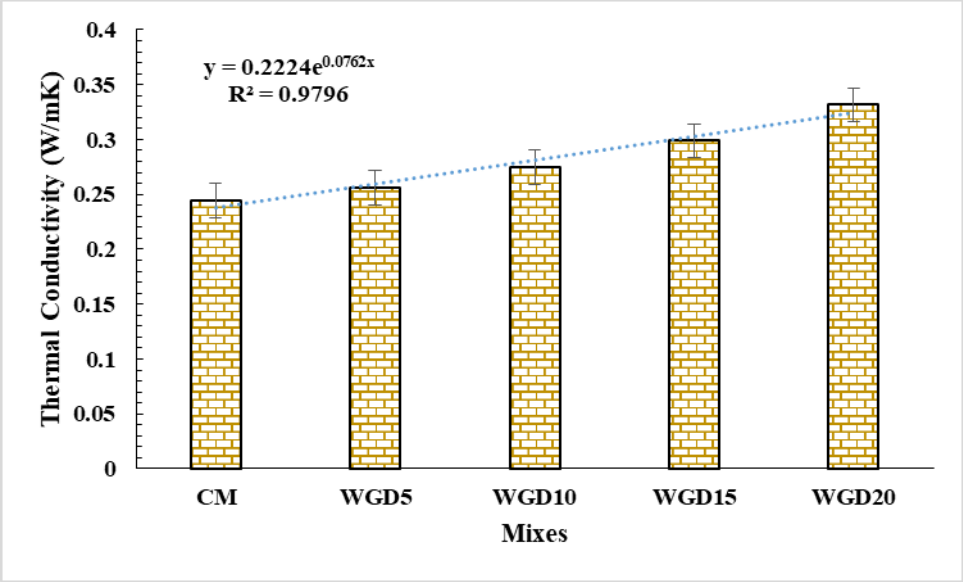

Figure 4. 13: Thermal conductivity of AAC mixes

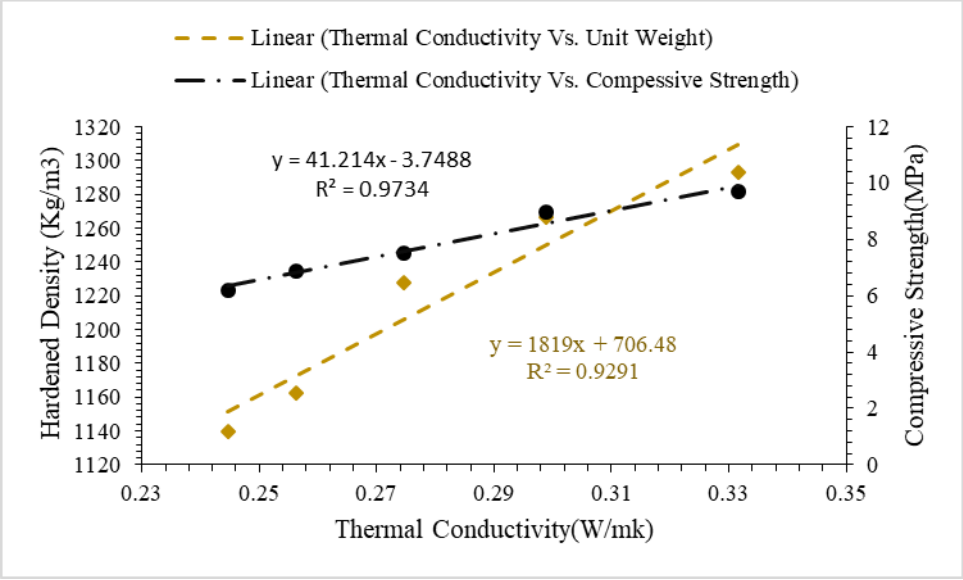

Figure 4. 14: Relationship between thermal conductivity, density and compressive strength

CHAPTER 5: CONCLUSIONS AND RECOMMENDATIONS

5.1. Conclusions

Incorporation of waste granite dust in AAC concrete has eco-friendly aspects that includes reduction of granite industry waste and beneficial impacts on physio-mechanical properties of AAC by virtue of physical effects (micro-filling, clogging) and chemical contribution through enhanced microstructure of cement paste matrix due to pozzolanic reaction. Therefore, detailed conclusions regarding the discussed properties of AAC containing waste granite dust are as follows:

a) Characterization results have shown that the waste granite dust (WGD) particles are rough, angular and flaky containing higher concentration of silica with the average particle size of 15.08 µm, whereas, quick lime is rich in reactive CaO concentration with particle size of 1.06 µm.
b) The compressive strength and hardened density of AAC increased while water absorption and porosity decreased with the incorporation of waste granite dust. The maximum compressive strength was observed in WGD20 which was 42% higher than that of CM mix. The maximum hardened density value of 1293.32 Kg/m^3 was achieved by WGD20 mix.
c) The thermal conductivity of WGD incorporated AAC increased as it is proportional to hardened density and enhanced microstructure.
d) From micro-structural analysis, it is evident that the addition of waste granite dust resulted in densely packed and foiled/plate like tobermorite crystals. The densified microstructure increased the physio-mechanical properties of AAC.
e) Thermogravimetric analysis revealed the extent of pozzolanic activity of WGD incorporated AAC by determining the concentration of portlandite. Lowest values of weight loss were observed in portlandite region for WGD10 and WGD20 mixes comparative to the CM mix. This indicated higher pozzolanic activity for AAC mixes with higher WGD content.
f) It is observed from the acid attack results that weight loss and strength loss due to sulfuric acid was higher as compared to the hydrochloric acid exposure because of more aggressive nature of sulfuric acid The decrease in density due to weight loss

observed for sulphuric acid exposure was higher than that of hydrochloric acid exposure. Furthermore the decrease in strength for sulphuric and hydrochloric acid was observed as 54% and 32.40%, respectively.

5.2. Recommendations

- The incorporation of waste granite dust in AAC with varying curing temperature and pressure can be further studied.
- It is recommended to study the incorporation of locally available waste materials to address the local waste management problems.

References

A Bonakdar, F.B., B Mobasher, 2013. Physical and mechanical characterization of fiber-reinforced aereted concrete (FRAC). Cement & Concrete Composites 38, 82-91.

A. Arivumangai1, T.F., 2014. Strength and Durability Properties of Granite Powder Concrete. Journal of Civil Engineering Research, 2163-2316

Albayrak, M., Yörükoğlu, A., Karahan, S., Atlıhan, S., Aruntaş, H.Y., Girgin, İ., 2007. Influence of zeolite additive on properties of autoclaved aerated concrete. Building and environment 42(9), 3161-3165.

Asadi Shamsabadi, E., Ghalehnovi, M., De Brito, J., Khodabakhshian, A., 2018. Performance of Concrete with Waste Granite Powder: The Effect of Superplasticizers. Applied Sciences 8(10), 1808.

ASTM-C109 / C109M-02, 2002. Standard Test Method for Compressive Strength of Hydraulic Cement Mortars (Using 2-in. or [50-mm] Cube Specimens), .

ASTM C150-04, 2004,. Standard Specification for Portland Cement, . ASTM International,.

ASTM C177-13, 2013,. Standard Test Method for Steady-State Heat Flux Measurements and Thermal Transmission Properties by Means of the Guarded-Hot-Plate Apparatus,. ASTM International, .

ASTM C267-01(2012), Standard Test Methods for Chemical Resistance of Mortars, Grouts, and Monolithic Surfacings and Polymer Concretes,. ASTM International,, West Conshohocken, PA, 2012,.

ASTM C348-18, 2018. Standard Test Method for Flexural Strength of Hydraulic-Cement Mortars,. ASTM International, , West Conshohocken, PA, .

ASTM C642-13, 2013. Standard Test Method for Density, Absorption, and Voids in Hardened Concrete, . ASTM International.

ASTM E2651-13, 2013. Standard Guide for Powder Particle Size Analysis, ASTM International

B962-17, A., 2017. Standard Test Methods for Density of Compacted or Sintered Powder Metallurgy (PM) Products Using Archimedes' Principle. ASTM International, West Conshohocken, PA.

BS1881-122, 2011. Method for determination of water absorption of Testing concrete.

C618-17a, A., 2017. Standard Specification for Coal Fly Ash and Raw or Calcined Natural Pozzolan for Use in Concrete, , ASTM International,.

Cong, X., Kirkpatrick, R.J., 1996. 29Si MAS NMR study of the structure of calcium silicate hydrate. Advanced Cement Based Materials 3(3-4), 144-156.

Dey, V., Bonakdar, A., Mobasher, B., 2014. Low-velocity flexural impact response of fiber-reinforced aerated concrete. Cement and Concrete Composites 49, 100-110.

Felixkala, T., & Partheeban, P. , 2010. Granite powder concrete. Indian Journal of science and Technology 3(3), 311-317.

Ghannam, S., Najm, H., Vasconez, R., 2016. Experimental study of concrete made with granite and iron powders as partial replacement of sand. Sustainable Materials and Technologies 9, 1-9.

Gupta, L.K., Vyas, A.K., 2018. Impact on mechanical properties of cement sand mortar containing waste granite powder. Construction and Building Materials 191, 155-164.

Hamza, R.A., El-Haggar, S., & Khedr, S. , 2011. Marble and granite waste: characterization and utilization in concrete bricks. International Journal of Bioscience, Biochemistry and Bioinformatics, 1(4), 286.

Hewlett, P., 2003. Lea's Chemistry of Cement and Concrete`, in: Hewlett, P. (Ed.) 4th ed.

HFW., T., 1997. Cement chemistry. 2nd ed. Thomas Telford Publishing;, London: .

Ho, D., Sheinn, A., Ng, C., Tam, C., 2002. The use of quarry dust for SCC applications. Cement and Concrete Research 32(4), 505-511.

Hong, S.-Y., Glasser, F., 2004. Phase relations in the CaO–SiO2–H2O system to 200 C at saturated steam pressure. Cement and Concrete Research 34(9), 1529-1534.

Kawai, K., Yamaji, S., Shinmi, T., 2005. Concrete deterioration caused by sulfuric acid attack, International Conference on Durability of Building Materials and Components. LYON [France]. pp. 17-20.
Kunchariyakun, K., Asavapisit, S., Sinyoung, S., 2018. Influence of partial sand replacement by black rice husk ash and bagasse ash on properties of autoclaved aerated concrete under different temperatures and times. Construction and Building Materials 173, 220-227.
Kunchariyakun, K., Asavapisit, S., Sombatsompop, K., 2015. Properties of autoclaved aerated concrete incorporating rice husk ash as partial replacement for fine aggregate. Cement and Concrete Composites 55, 11-16.
Kunchariyakun, K., Asavapisit, S., & Sombatsompop, K., 2015. Properties of autoclaved aerated concrete incorporating rice husk ash as partial replacement for fine aggregate. Cement and Concrete Composites 55, 11-16.
Kurama H, T.I., Karakurt C., 2009. Properties of the autoclaved aerated concrete production from coal bottom ash. J Mater Process Tech, 767–773.
Lakhani, R., Kumar, R., Tomar, P., 2014. Utilization of Stone Waste in the Development of Value Added Products: A State of the Art Review. Journal of Engineering Science & Technology Review 7(3).
Mansoor, Y., Syed, N.A., 2012. Pakistan Marble Industry Challenges: Opportunities for China in Pakistan. Journal of Independent Studies and Research 10.
Memon, S.A., Javed, U., Khushnood, R.A., 2019. Eco-friendly utilization of corncob ash as partial replacement of sand in concrete. Construction and Building Materials 195, 165-177.
Mendoza, J.-M.F., Feced, M., Feijoo, G., Josa, A., Gabarrell, X., Rieradevall, J., 2014. Life cycle inventory analysis of granite production from cradle to gate. The International Journal of Life Cycle Assessment 19(1), 153-165.
Menezes, R.R., Ferreira, H.S., Neves, G.A., Lira, H.d.L., Ferreira, H.C., 2005. Use of granite sawing wastes in the production of ceramic bricks and tiles. Journal of the European Ceramic Society 25(7), 1149-1158.
Mitsuda, T., Toraya, H., Okada, Y., Shimoda, M., 1988. Synthesis of tobermorite: NMR spectroscopy and analytical electron microscopy, Advanced Characterisation Techniques for Ceramics Proc. 41 st Pacific Coast Reg. Mtg. American Ceramic Society, San Francisco, 24-26 October 1988. pp. 206-213.
Montani, C., 2016. XXVII World Marble and Stones Report 2016. Aldus Casa di Edizioni in Carrara.
Mostafa, N., 1995. Factors effecting the hydrothermal reactions in CaO±SiO2±H2O system. MSc thesis, Suez Canal University.
Mostafa, N., 2005. Influence of air-cooled slag on physicochemical properties of autoclaved aerated concrete. Cement and Concrete Research 35(7), 1349-1357.
Mostafa, N., El-Hemaly, S., Al-Wakeel, E., El-Korashy, S., Brown, P., 2001. Activity of silica fume and dealuminated kaolin at different temperatures. Cement and Concrete Research 31(6), 905-911.
Narayanan, N., & Ramamurthy, K. , 2000. Microstructural investigations on aerated concrete. Cement and Concrete Research 30(3), 457-464.
Narayanan, N., Ramamurthy, K., 2000. Structure and properties of aerated concrete: a review. Cement and Concrete Composites 22(5), 321-329.
Newman, J., Choo, B.S., 2003. Advanced concrete technology 3: processes. Elsevier.
P. Kumar Mehta, P.J.M.M., 2006. Concrete: Microstructure, properties and Materials, Third Edition ed. McGraw-Hill, USA.
Pareek, S., 2007. Gainful Utilization of Marble Waste–An Effort towards Protection of Ecology & Environment. Centre for Development of Stones. Retrieved: http://www. cdos-india. com/Papers% 20 technical. htm.
Pellenq, R.J.-M., Kushima, A., Shahsavari, R., Van Vliet, K.J., Buehler, M.J., Yip, S., Ulm, F.-J., 2009. A realistic molecular model of cement hydrates. Proceedings of the National Academy of Sciences 106(38), 16102-16107.

R. Siddique, Y. Aggarwal, P. Aggarwal, E.H. Kadri, Bennacer, R., 2011. Strength, durability, and micro-structural properties of concrete made with used-foundry sand (UFS). Constr. Build. Mater. 25, 1916-1925.
Ramos, T., Matos, A.M., Schmidt, B., Rio, J., Sousa-Coutinho, J., 2013. Granitic quarry sludge waste in mortar: Effect on strength and durability. Construction and Building Materials 47, 1001-1009.
Rego, G., Martínez, C., Quero, A., Blanco, T.P., Borquea, J., 2001. The effects of dust inhalation in slate industry workers. Medicina clinica 116(8), 290-291.
Różycka, A., & Pichór, W. (2016), 2016. Effect of perlite waste addition on the properties of autoclaved aerated concrete. Construction and Building Materials 120, 65-71.
Saboya Jr, F., Xavier, G., Alexandre, J., 2007. The use of the powder marble by-product to enhance the properties of brick ceramic. Construction and Building Materials 21(10), 1950-1960.
Sadek, D.M., El-Attar, M. M., & Ali, H. A., 2016. Reusing of marble and granite powders in self-compacting concrete for sustainable development. Journal of Cleaner Production 121, 19-32.
Sato, H., Grutzeck, M., 1991. Effect of starting materials on the synthesis of tobermorite. MRS Online Proceedings Library Archive 245.
Schober, G., 2005. The most important aspects of microstructure influencing strength of AAC. AAC, Taylor & Francis, hal, 145-153.
Siddique, R., 2003. Effect of fine aggregate replacement with Class F fly ash on the mechanical properties of concrete. Cement and Concrete Research 33, 539-547.
Singh, S., Nagar, R., Agrawal, V., Rana, A., & Tiwari, A. , 2016. Sustainable utilization of granite cutting waste in high strength concrete. Journal of Cleaner Production 116, 223-235.
Stutzxnan, P.E., & Centeno, L., 1995. Compositional analysis of beneficiated fly ashes. National Institute of Standards and Technology Interagency Report, USA.
Thomas, B.S., Gupta, R.C., Kalla, P., Cseteneyi, L., 2014. Strength, abrasion and permeation characteristics of cement concrete containing discarded rubber fine aggregates. Construction and Building Materials 59, 204-212.
Van Rooyen, A.S., 2013. Structural lightweight aerated concrete. Stellenbosch: Stellenbosch University.
Wiedmann, T.O., Schandl, H., Lenzen, M., Moran, D., Suh, S., West, J., Kanemoto, K., 2015. The material footprint of nations. Proceedings of the National Academy of Sciences 112(20), 6271-6276.
Wongkeo, W., Chaipanich, A., 2010. Compressive strength, microstructure and thermal analysis of autoclaved and air cured structural lightweight concrete made with coal bottom ash and silica fume. Materials Science and Engineering: A 527(16-17), 3676-3684.
Xu, W., Lo, Y.T., Ouyang, D., Memon, S.A., Xing, F., Wang, W., Yuan, X., 2015. Effect of rice husk ash fineness on porosity and hydration reaction of blended cement paste. Construction and Building Materials 89, 90-101.